STUDIES ON POLARIZATION MULTIPLEXED TRANSMISSION SYSTEM

A Project Report

submitted by

ANEESH. S

in partial fulfilment of the requirements
for the award of the degree of

MASTER OF TECHNOLOGY

DEPARTMENT OF ELECTRICAL ENGINEERING
INDIAN INSTITUTE OF TECHNOLOGY MADRAS.

MAY 2014

THESIS CERTIFICATE

This is to certify that the thesis titled **Studies on Polarization Multiplexed Transmission System**, submitted by **Aneesh. S**, to the Indian Institute of Technology, Madras, for the award of the degree of **Master of Technology** (Photonics) in Electrical Engineering, is a bona fide record of the research work done by him under my supervision. The contents of this thesis, in full or in parts, have not been submitted to any other Institute or University for the award of any degree or diploma.

Dr. Deepa Venkitesh
Research Guide
Assistant Professor
Dept. of Electrical Engineering
IIT-Madras, 600 036

Place: Chennai

Date: 6th May 2014

ACKNOWLEDGEMENTS

I would like to express my deep sense of gratitude and regards to my guide Dr. Deepa Venkitesh, for her guidance, invaluable support, encouragement and great interest throughout the execution of the research work.

I would like to thank all the Photonics (EE5) faculties for their valuable support through out my work.

I thank my Ocean Lab mates and friends Aravind P. Anthur, Sai Krishna, Ravi Kiran, and Smaranika Swain for the informative discussions and memorable times in the lab.

I also thank all the Fil Lab and Expo Lab members and friends for their support throughout the research period.

I wish to acknowledge with gratitude and appreciation to Optellent Inc. for providing the BERT and Sterilite Technologies Ltd. for providing the fiber for measurements.

ABSTRACT

KEYWORDS: Dispersion tolerance; Optical duobinary; Polarization Division Multiplexing ; Polarization Mode Dispersion; spectral efficiency.

Demand for greater bandwidth to home grows continuously and so research has been focused on developing new optical access network architectures to satisfy the bandwidth demands. In addition to the band width, another significant trend in access network is to achieve longer reach. Polarization effects in light wave system is a big concern when we think about long reach and higher band width. One of the promising and easy way to double the bandwidth without doubling the bandwidth of the electronics is to use a polarization division multiplexing scheme. Then we need to be more concern about PMD impairment. For long reach networks another difficulty is the SBS threshold of the fiber which will set a higher power level that can be launched into the fiber. So we study these three aspects here PMD, PDM system and SBS threshold of PDM signals.

In this thesis we present the simulation results of the PMD induced penalty in different operating conditions like bitrates, fiber length and modulation format. We report the OSNR penalty in each case. We also describe the simulation and experimental results to demonstrate the better performance of Polarization Division Multiplexed Optical Duobinary (PDM-ODB) modulation format in terms of OSNR requirement for propagation of upto 100 km with an effective data rate of 20 Gbps. In this thesis we also investigate the SBS threshold of PDM signals.

TABLE OF CONTENTS

LIST OF TABLES

LIST OF FIGURES

ABBREVIATIONS

APD	Avalanche Photo Diode
ASE	Amplified Spontaneous Emission
BER	Bit Error Rate
BERT	Bit Error Rate Tester
B2B	Back to Back
BPSK	Binary Phase Shift Keying
CD	Chromatic Dispersion
CW	Continuous Wave
CSRZ	Carrier-Suppressed Return-to-Zero
CNLSE	Coupled Non-Linear Schrodinger Equation
DPSK	Differential Phase Shift Keying
DGD	Differential Group Delay
DFB	Distributed Feed Back
EDFA	Erbium Doped Fiber Amplifier
FEC	Forward Error Correction
FFT	Fast Fourier Transform
FIR	Finite Impulse Response
HNLF	Highly Non-Linear Fiber
IFFT	Inverse Fast Fourier Transform
ISI	Inter Symbol Interference
LPF	Low Pass Filter
NRZ	Non Return to Zero
ODB	Optical DuoBinary
OFDM	Orthogonal Frequency Division Multiplexing
OOK	On-Off Keying
OSNR	Optical Signal to Noise Ratio
OSA	Optical Spectrum Analyzer
PC	Polarization Controller

PMD	Polarization Mode Dispersion
PDM	Polarization Division Multiplexing
PM-DQPSK	Polarization Multiplexed Differential Quadrature Phase Shift Keying
PSP	Principal State of Polarization
PBS	Polarization Beam Splitter
PBC	Polarization Beam Combiner
PRBS	Pseudo Random Bit Sequence
PON	Passive Optical Network
QAM	Quadrature Amplitude Modulation
RZ	Return-to-Zero
SBS	Stimulated Brillouin Scattering
SSFM	Split Step Fourier Transform
SPM	Self Phase Modulation
SOA	Semiconductor Optical Amplifier
SOP	State Of Polarization
SNR	Signal to Noise Ratio
SMF	Single Mode Fiber
TBPF	Tunable Band Pass Filter
VOA	Variable Optical Attenuator
WDM	Wavelength Division Multiplexing
XPM	Cross Phase Modulation

NOTATION

$\triangle\tau$	Differential Group Delay
R	Rotational Matrix
$< \triangle\tau >$	Average DGD
θ	Azimuth Angle
ϵ	Angle of Ellipticity
D	Diagonal Matrix
$\triangle\beta_0$	Frequency independent birefringence
$\triangle\beta_1$	Differential phase shift induced by PMD
$\vec{\sigma}$	spin vector
$\hat{i}\,(z)$	unit magnitude real vector (a stokes vector)
P_D	PMD coefficient of the fiber
ω	Carrier Frequency
B_{ref}	Reference Bandwidth
E_x	Electric field in x polarization
E_y	Electric field in y polarization
A_{eff}	Effective cross sectional area of propagating wave
$\triangle\nu_{SBS}$	Spontaneous Brillouin bandwidth
$\triangle\nu_p$	Pump light bandwidth
κ_{SBS}	Polarization factor
L_{eff}	effective interaction length
α	attenuation of the fiber in m^{-1}
f_0	Spectral bandwidth

CHAPTER 1

INTRODUCTION

1.1 Introduction

There has been increasing demand for the traffic capacity due to the increasing use of voice, video and data in optical communication systems. The capacity explosions of optical fiber links have taken place due to the techniques such as Wavelength Division Multiplexing (WDM). With this technique it is difficult to accommodate for smaller wavelength channel spacing and wider wavelength ranges due to many factors such as optical filters, wavelength shifts, signal bandwidth, EDFA bandwidth, dispersion and nonlinearities. One of the readily accepted techniques for the maximum utilization of the available bandwidth is Polarization Division Multiplexing (PDM). Here independent signals are simultaneously transmitted in two orthogonal polarizations. PDM signals can be then carried over WDM, thus, increasing the capacity two-fold. The major problems with PDM are the coherent cross talk due to misaligned polarizers or polarization beam splitters (PBS) and that due to polarization mode dispersion (Nelson and H.Kogelnik, 2000). Mitigation of the PMD is very important for the practical implimentation of PDM and hence people have come up with all optical signal regeneration schemes (A.L.Yi *et al.*, 2011) with a polarization diversified loop using HNLF which proved its ability to mitigate PMD to certain extent. PDM is generally used in conjunction with advanced modulation formats like PM-DQPSK, which are in a way resistant to polarization related issues in data transmission.

With the increase in bitrate, light wave systems are found to be more sensitive to polarization mode dispersion. So, PMD has been a subject matter of research even before PDM got implemented. Study on the system tolerance to PMD, with different modulation formats says that PMD induced OSNR penalty is less for chirped RZ formats and duobinary modulation formats compared to NRZ (C.Xie *et al.*, 2003). Similarly, compared to NRZ, PMD induced inter symbol interference (ISI) is less for DPSK (C.Xie *et al.*, 2003). Jopson and Nelson studied the NRZ and RZ modulated signals and its

PMD induced impairment (Jopson *et al.*, 1999) and they found that RZ is more robust to PMD impairment as compared to NRZ.

We also propose a long-reach access network using PDM systems. The benefit of the increased bandwidth and spectral efficiency with the use of advanced modulation formats in the long-haul core networks can be passed on directly to the customers by bypassing the metro networks and directly resorting to long-reach optical access networks. Passive optical links with longer reach reduces the bottle neck due to the optical-electrical-optical conversion in the metro nodes and switches, thus providing an increased bandwidth with improved cost and energy efficiency. This idea was first demonstrated with a 100 km long-reach access link with 1024 nodes with 10 Gbps data rates with OOK modulation format in 2007 (D.P.Shea and J.E.Mitchell, 2007). Amplifiers are included in such networks for extending the reach, thus making them not strictly passive. There has been a recent study on the use of digital coherent receivers for long-reach access networks (D.Lavery *et al.*, 2013). Countering fiber dispersion without the use of electronic dispersion compensator or digital processing is one of the challenges in such long-reach networks. Optical duobinary (ODB) modulation format has been well known for its dispersion tolerance (T.Franck *et al.*, 1996) because of its smaller spectral width and hence it is an attractive format which could be adopted for such networks (J.D.Downie *et al.*, 2009). Increased spectral efficiency is another aspect of interest. Increased reach of upto 350 km was demonstrated in the past with the use of PDM-ODB format with dispersion compensation and active control of polarization (P.Boffi *et al.*, 2008).

In this work we demonstrate the experimental implementation and the dispersion resilience of the aforementioned PDM-ODB technique without an extra penalty compared to the single polarization system for a propagation length of up to 100 km length of fiber. The BER performance of PDM-NRZ, single polarization ODB and PDM-ODB are compared when 10 Gbps data is propagated through different lengths of fiber. The reduced OSNR requirements with the use of PDM-ODB compared to PDM-NRZ format are demonstrated. The proposed system could thus be used for increased spectral efficiency without including any active elements in the system, for long-reach access networks.

1.2 Organization of the thesis

Chapter. 1 gives an introduction to polarization mode dispersion. It also describes the PDM system and its relevance in long reach access network. Chapter. 2 describes the Polarization Mode Dispersion in detail and the results of simulation on the effects of PMD on different modulation formats and bit rates. The simulation on the effect of dispersion and nonlinearities with a PDM system for different modulation formats are described further in Chapter. 3. Chapter. 4 describes the Experimental setup of PDM-NRZ and PDM-ODB system and the analysis of PDM experimental results in detail. Chapter. 5 gives an introduction of the SBS threshold related previous works and its importance in long haul communication systems. Then describes the theoretical calculation of SBS threshold of CW, NRZ and ODB signals. Finally it explains the experimental setup to find out the threshold in single polarization and PDM systems and analyses the experimental results. Chapter. 6 concludes with the works done and gives the scope for future work.

CHAPTER 2

POLARIZATION MODE DISPERSION

2.1 Introduction

Polarization mode dispersion is one of the major impairments in the high speed optical communication.This impairment is more severe in the network operating at a data rate of more than 10 Gbps. PMD occurs when fiber birefringence causes a signal propagating through the fiber to experience a polarization dependent group delay (Jopson *et al.*, 1999). Optical pulses propagate in an optical fiber with a speed determined by its refractive index. If the fiber was absolutely symmetrical the speed of light should not depend on the polarization of the light. But the refractive indices in the X and Y directions are different in actual fibers and this difference is called birefringence. Thus the speed of light in the fiber becomes dependent on the polarization.

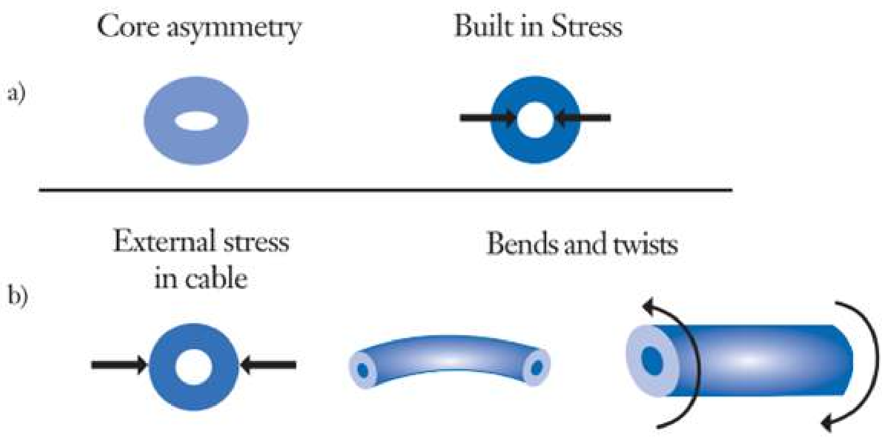

Figure 2.1: Causes of birefringence in the fiber(source: White paper,Corning)

The different causes of birefringence in the fiber are shown in Fig. 2.1. It can be arised due to core asymmetry or can be introduced through internal stresses during manufacturing fiber, or through external stresses during cabling and installation. Any non-uniform loading of the fiber cross-section, or bends or twists that are introduced to the fiber will result in an external stress on to the fiber (S.Ten and M.Edward, 2006). First order PMD is the distortion that exhibits a behavior similar to that of simple birefringence; it causes the input polarization to rotate in Stokes space about a single axis.

Any incident signal can be projected into orthogonal principle state of polarizations (PSP) and the two orthogonal states experience different delay. The difference in the transmission delay between two PSPs is called Differential Group Delay (DGD) shown in Fig. 2.2 and is usually denoted as $\triangle\tau$. A signal launched exactly to the PSP will not suffer any first order PMD impairments (Jopson *et al.*, 1999). In higher order PMD, the birefringence is modeled as a Stokes vector with linear frequency dependence and it causes random mode coupling (Serena, 2009). Generally we use coupled nonlinear Schrodinger equation (CNLSE) in its vector form (equation. 2.1) to model the PMD impairments in the fiber.

$$\begin{aligned}\frac{\delta A(z,\tau)}{\delta z} &= \frac{\alpha}{2}A - i\frac{\triangle\beta_0}{2}\left(\hat{i}(z).\vec{\sigma}\right)A - \frac{\triangle\beta_1}{2}\left(\hat{i}(z).\vec{\sigma}\right)\frac{\delta A}{\delta\tau} \\ &+ i\frac{\beta_2}{2}\frac{\delta^2 A}{\delta\tau^2} - i\gamma\left[|A|^2 A - \frac{1}{3}\left(A^T\sigma_3 A\right)\sigma_3 A\right]\end{aligned} \tag{2.1}$$

Where A denotes the complex electric fields; $A = [A_x, A_y]^T$

α- attenuation i.e; the power loss along the distasnce

$\triangle\beta_0$- Frequency independent birefringence.

$\triangle\beta_1$- differential phaseshift induced by the PMD; $\triangle\beta_1 = DGD_{rms} \times \omega$

$\triangle\beta = \beta_{slow}(\omega) - \beta_{fast}(\omega)$, strength of birefringence which has both frequency dependent and frequency independent term

$\beta_k = \frac{d^k\beta}{d\omega^k}\mid_{\omega=\omega_0}$, where ω_0 is the central frequency of $A(z,t)$.

γ- Non-linear coefficient.

$\vec{\sigma}$- (a tensor) spin vector whose elements are spin matrices.

$\left(\hat{i}(z).\vec{\sigma}\right)$- scalar product yields a unitary Jones matrix which acts on the elements of Electric field A and produces mode coupling,

$\hat{i}(z)$- unit magnitude real vector (a Stokes vector).

The Pauli matrices are,

$\sigma_0 = \begin{bmatrix} 1 & 0 \\ 0 & 1 \end{bmatrix}, \sigma_2 = \begin{bmatrix} 0 & 1 \\ 1 & 0 \end{bmatrix}, \sigma_3 = \begin{bmatrix} 0 & -i \\ i & 0 \end{bmatrix}.$

The computational time required for solving the CNLSE is large and hence Manakov introduced a simpler equation known as Manakov PMD equation (Marcuse and Menyukl, 1997) given by equation. 2.2 .

$$\frac{\delta A(z,\tau)}{\delta z} = \frac{\alpha}{2}A - i\frac{\triangle\beta_0}{2}\left(\hat{i}(z).\vec{\sigma}\right)A - \frac{\triangle\beta_1}{2}\left(\hat{i}(z).\vec{\sigma}\right)\frac{\delta A}{\delta\tau} + i\frac{\beta_2}{2}\frac{\delta^2 A}{\delta\tau^2} - i\gamma\frac{8}{9}|A|^2 A \tag{2.2}$$

Solution of this equation requires much smaller computational time compared to CNLSE. It averages the impact of signal polarization over the nonlinear term in equation. 2.1 and we can see the only difference in equation. 2.2 is the last nonlinear term, $\frac{8}{9}\gamma| A |^2 A$ which includes the effect of Ker nonlinearity averaged over the Poincare sphere with the well known 8/9 factor (Serena, 2009).

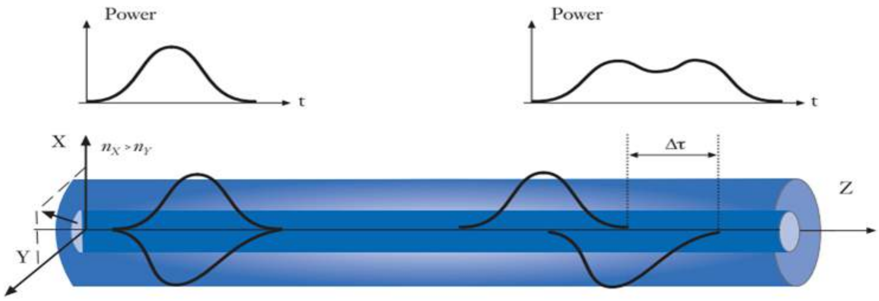

Figure 2.2: A pulse seperation into x and y axix due to DGD at output (source: White paper, Corning)

PMD and DGD are related in more complex way as the fiber birefringence varies along the length both in terms of refractive index asymmetry and the relative orientation of slow and fast axis. So to understand the nature of PMD we should represent fiber as concatenation of birefringent sections of fiber coupling by coupling sites as shown in Fig. 2.3.

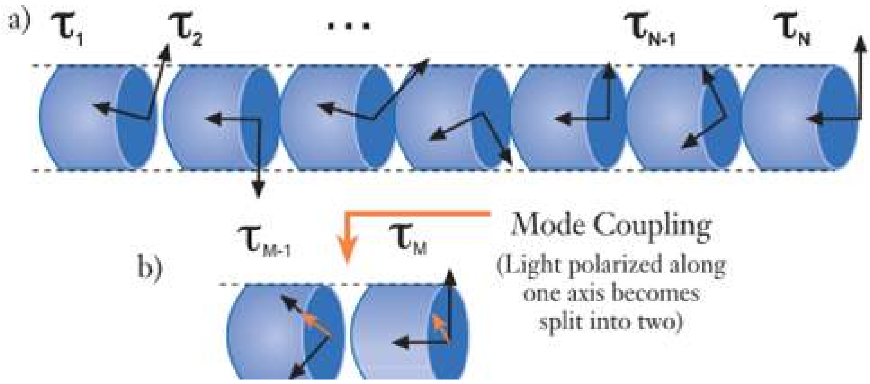

Figure 2.3: Physical model of fiber PMD as a concatenated series of birefringent fiber sections (source: White paper, Corning)

If we measure instantaneously the value of DGD at output of the fiber, it would be a random value. Histograms of repeated DGD measurements shows that it follows a "Maxwellian" statistics. From the statistics the average DGD or $< \triangle\tau >$ is known as the PMD of the fiber (S.Ten and M.Edward, 2006). Numerous experiments with fibers of different lengths have shown that PMD of fiber is proportional to the square root of the fiber length.

$$PMD =< \triangle\tau >= PMD_{Coeff}\sqrt{L} \tag{2.3}$$

The PMD_{Coeff} is the parameter usually available in the specifications of the commercial fiber. For G652 the value of PMD_{Coeff} is $0.5ps/\sqrt{km}$.

2.2 Simulation

We have used Optilux Software for simulating the PMD in fiber. Optilux is an open source package containing collection of Mat lab functions. The algorithm used for simulating the PMD in optical fiber was studied. It solves the PMD-Manakov equation (equation. 2.2) using basic vectorial Split Step Fourier Transform Method, but the step size used is not constant; it varies with different power (at different length of the fiber). First we calculate the nonlinear step size and we apply the nonlinear effects. Before applying the linear effects (GVD,DGD and birefringence) we divide each wave plates into many number of trunks (equivalent to PMF) and apply the linear part of the SSFM into each trunks. Thus the whole length of the fiber is divided as shown in Fig. 2.4 for the PMD evolution. Algorithm in detail is given in Appendix. A.

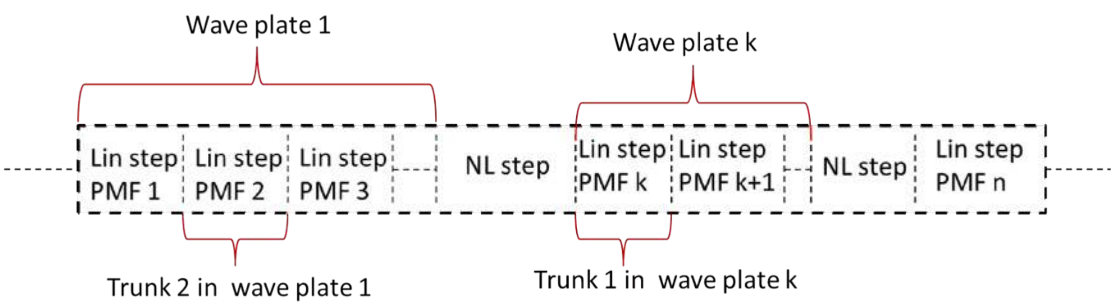

Figure 2.4: Fiber length is devided into waveplates and trunks for simulating PMD effects; NL step: Non-Linear step, Lin step: Linear step, PMF: Polarization Maintaining Fiber

2.3 Simulation results

First we studied the basic impact of PMD in the pulse propagation. For that we used a 40 Gbps data and introduced both first order PMD and higher order PMD in the simulation. We used 100 km fiber with the impairment as PMD alone. The PMD coefficient of the fiber is, $P_D = 0.5ps/\sqrt{km}$. Average DGD (ps) = $P_D \times \sqrt{L}$, where L is the length of the fiber in km. In simulation we used normalized DGD= AverageDGD/ bit period, where bit period=1/bit rate. The results are as shown below. We initialized our simulation with the data only in the x polarization and made y polarized component zero. At the end of the 100 km fiber we could see power both in x and y components. The Transmitted and received total power is shown in Fig. 2.5. At 40 Gbps, a fiber length of 100 km introduces an average DGD (normalized to bitrate) of 0.2 symbols. In these conditions higher order PMD is not that significant enough to produce pulse distortion. However the first order PMD causes a pulse broadening which leads to inter symbol interference (ISI). In Fig. 2.5, we can see the received total power has a small pulse broadening (0.2 bits).

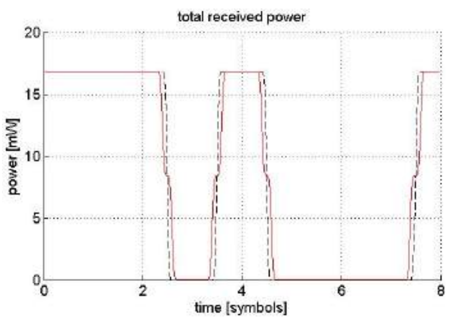

(a) First order PMD case

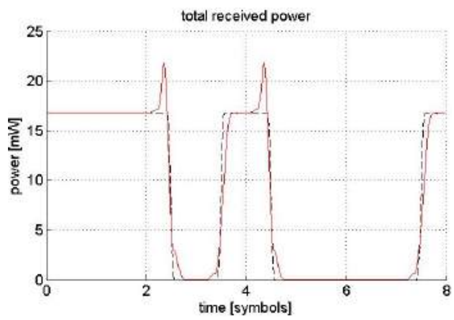

(b) Higher order PMD case

Figure 2.5: Transmitted power (black color dotted) and total received power (red) at the output of 100 km, higher order PMD

In Fig. 2.6, the plots show the splitting of each pulse into two shadow pulses, due to first order PMD, as it propagate along the fiber. These pulses (corresponding to x and y polarization) arrive at the fiber end with a mutual delay. In higher order PMD "random mode coupling", i.e., the exchange of energy between the field components causes a distortion of the pulse shapes and hence the signal will undergo both signal degradation and ISI (Serena, 2009). In Fig. 2.6, the plots "Total x power" and "Total y power" show the random coupling between x and y field components and hence a pulse distortion when higher order PMD is included in the simulation.

In equation. 2.2, the birefrengence is modeled by a Stokes vector,

$$\vec{W}(z,\omega) = (\triangle\beta_0 + \triangle\beta_1\omega)\,\hat{i}(z)$$

with a linear frequency dependence (Serena, 2009). The variation in z of its orientation cause "random mode coupling". If $\hat{i}$ is constant along z, random mode coupling will not happen and it evokes only first order PMD as shown in Fig. 2.6 (a) & (c) without pulse distortion. If $\hat{i}$ (stokes vector) is not constant along the length of the fiber, then in addition to the ISI, the pulse distortion also happen because of the higher order PMD as shown in Fig. 2.6 (b) & (d). It is also noticed that the y component is present in the entire pulse width. This is because of non zero value of frequency independent term $\triangle\beta_0$, and the overshoot is happening at the rising and falling edges due to frequency dependend term $\triangle\beta_1$ which in turn in the time domain gives time derivative. At the output we will get y components only in rising and falling edges of the pulses in the first order PMD case if we give the frequency independent birefringence $\triangle\beta_0 = 0$. This is due to the presence of only the frequency dependent term $\triangle\beta_1(\omega)$ in the total birefringence.

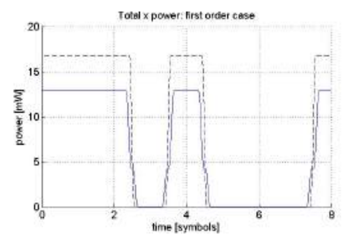

(a) x polarization power :First order PMD

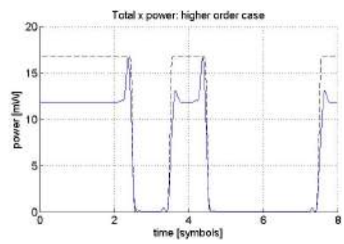

(b) x polarization power :Higher order PMD

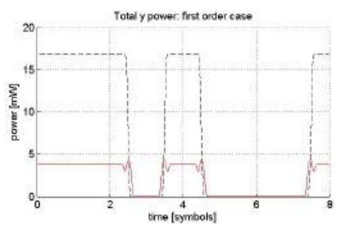

(c) y polarization power: First order PMD

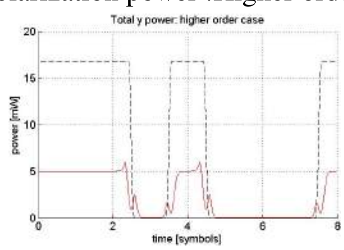

(d) y polarization power: Higher order PMD

Figure 2.6: (a) & (c) show the evolution of both x and y polarization power after, affected by first order PMD. (b) & (d) show the evolution of both x and y polarization power, after affected by higher order PMD, when the fiber length was 100 km and datarate is 40 Gbps; dotted line in all these figures represent the total transmitted power.

2.3.1 Transmission impairments due to PMD in presence of CD, SPM and XPM

Now we study the transmission impairments due to PMD in the presence of chromatic dispersion (CD), self phase modulation (SPM) and cross phase modulation (XPM). We study the impairment using the metric OSNR penalty, for a BER of 10^{-9}. The parameters used for simulations are bit rate =10 Gbps (NRZ-OOK), length of the fiber = 142 km, calculated average DGD= 0.059. The back to back measurement (b2b) gives the OSNR of 13.25 dB/0.1nm in the above simulation. Based on the b2b result we calculated the penalty and is tabulated as below.

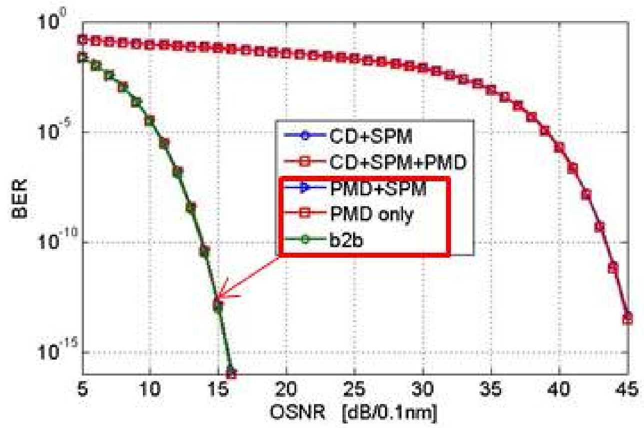

Figure 2.7: BER vs OSNR when the effects of CD, PMD and SPM is included. The bit rate used is 10 Gbps (OOK) and the length of the fiber is 142 km

Table 2.1: OSNR penalty with different system impairments

Impairments present	OSNR(dB/0.1nm)	OSNR penalty (dB)
CD+SPM+XPM	42.85	29.60
CD+SPM+XPM+PMD(1^{st}order)	42.77	29.52
With dispersion compensation PMD+SPM	13.33	0.08
With PMD only	13.29	0.04

In this study we restricted our fiber length to 142 km because of higher OSNR penalty (around 30 dB) when all the impairments are included. This is a representative length, good enough to get a rough idea about what is happening in each case. When PMD is introduced with the other impairments the penalty is reduced slightly. Thus PMD is not the major limitation at these length scales, especially in the presence of CD and nonlinearity induced impairments. At more stringent conditions i.e., at higher bit rates and at longer fiber lengths (since the average DGD is more) this effect can be clearer. Now to study the effects of PMD in a more standard way we assume that all other impairment except PMD is compensated. So further in all simulations we are assuming only the presence of PMD. For the penalty calculation we studied all possible back to back measurements, i.e., for different bitrates and for different modulation formats.

Table 2.2: Calculated values of OSNR at BER of 10^{-3} and 10^{-9} in the back to back systems

b2b OSNR (dB/0.1nm) for BER of 10^{-3}				
Bitrate(Gbps)	NRZ	50%RZ	33%RZ	67%RZ
10	7.99	7.29	8.57	7.29
28	12.46	11.76	13.04	11.76
40	14.01	13.31	14.59	13.31
100	17.99	17.29	18.57	17.29

b2b OSNR (dB/0.1nm) for BER of 10^{-9}				
Bitrate(Gbps)	NRZ	50%RZ	33%RZ	67%RZ
10	13.25	12.23	13.41	12.26
28	17.72	16.70	17.95	16.73
40	19.27	18.25	19.50	18.28
100	23.25	22.23	23.47	22.26

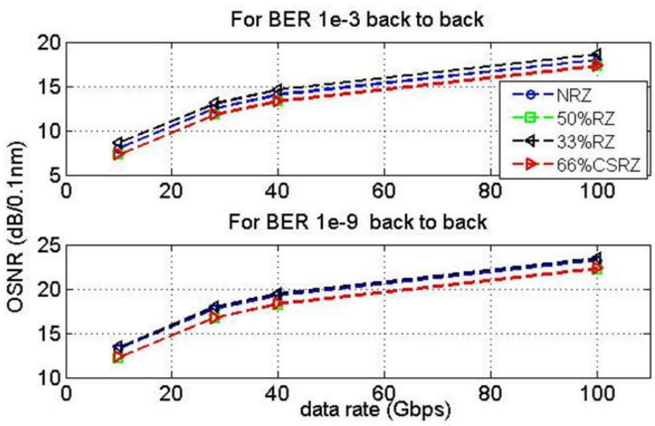

Figure 2.8: OSNR requirement for different data rates for NRZ, RZ and CRZ modulation formats

This values can be graphically shown as in Fig. 2.8. The results shows that even for b2b system, OSNR requirement increases as the bitrate increases. This can be justified directly from the definition of the OSNR.

$$OSNR = SNR \times \frac{baudrate}{2 \times B_{ref}} \tag{2.4}$$

Equation 2.4 tells that with baud rate (or bitrate) OSNR required for given BER increases.

2.3.2 PMD and bitrate

To study how the bit rates are related to the PMD impairment we ran a simulation fixing all other parameters same and changed the bitrates. We tried it with 100 km and 1000 km fiber.

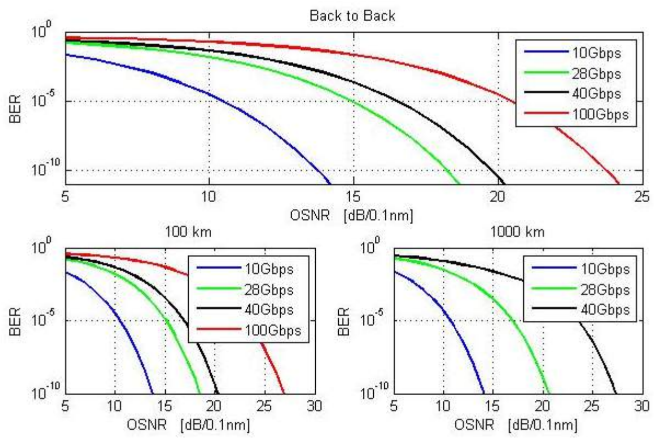

Figure 2.9: PMD impairment on bit rates (NRZ-OOK) at fiber lengths of 100 km and 1000 km

The OSNR penalty obtained from the above simulation with different bit rates is shown in Fig. 2.10. Here we did the simulation for first order PMD to see how different bit rate is affected by the PMD impairment and found out the OSNR penalty for obtaining a BER of 10^{-9} and 10^{-3} (which is used with Forward Error Correction (FEC)) at two fiber lengths 100 km and 1000 km.

Thus we can see that as the bit rate increases the OSNR penalty also increases. And it is more severe in the long haul communication (say 1000 km). First order PMD causes a penalty of 7.05 dB at 40 Gbps and even higher for 100 Gbps at this length. The higher order PMD is highly random and it is difficult to predict the exact penalty. So we ran simulation multiple times and took an average of the penalty introduced and we could clearly see that the randomness is more for higher bit rates and especially at larger fiber length.

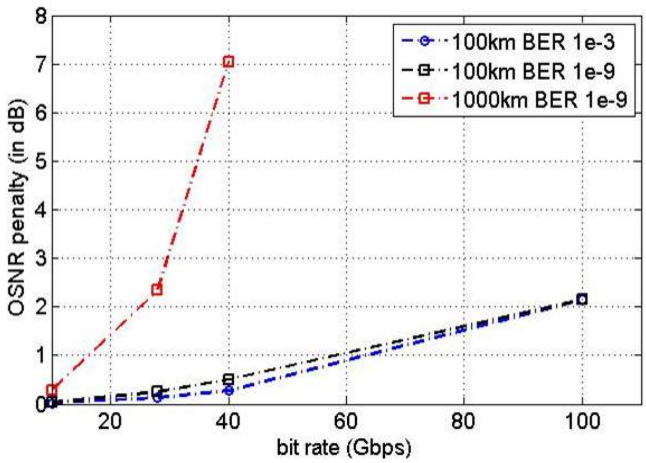

Figure 2.10: Bitrate and PMD impairment

2.3.3 Maximum optical reach of the system at different bit rate and at different OSNR penalty

We attempted to study the effect of PMD at different length of the fibers where we extended our fiber length to 4800 km to see the maximum reach of the system when only the PMD impairment is present.We saw that the PMD impairment is directly proportional to the square root of the length of the fiber and hence with fiber length the average DGD increases and so the OSNR penalty. The simulation result can be consolidated in a single graph which shows the OSNR penalty variation with the fiber lengths which we performed at different bit rates.

Here we limited our maximum penalty allowed to be below 30 dB and hence with the bitrate 40 Gbps maximum fiber length we could use is 2300 km at BER of 10^{-9} and 2400 km at BER of 10^{-3} . At 28 Gbps we could use up to 4800 km (BER10^{-9}), and we restricted our all simulation within 4800 km for plotting all the cases in a single graph. In practical situation, if allowed OSNR penalty is fixed to be 6 dB, then from Fig. 2.11 we can tell the reach is around 1200 km for 40 Gbps NRZ, 2500 km for 28 Gbps NRZ and for 10 Gbps the PMD effect is negligible.

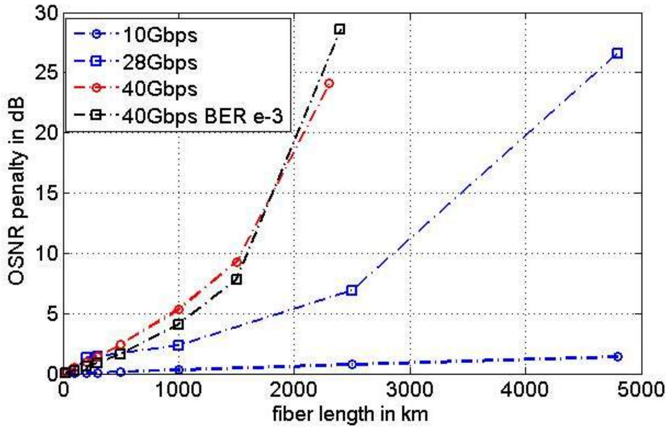

Figure 2.11: OSNR penalty vs. fiber length

2.3.4 PMD tolerance of RZ formats compared to NRZ

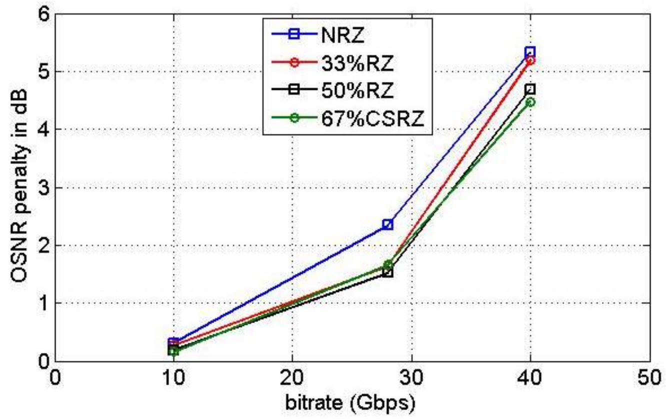

Figure 2.12: Comparing OSNR penalty for NRZ and RZ with different dutycycle

At different modulation formats PMD impairments are also different. We tried to study this problem also through simulation. As of now we are using only OOK, however studying different cases such as NRZ, 50% RZ, 33%RZ and 67%CSRZ. The simulation results are as shown in the Fig.2.12. The simulation was done with fiber length of 1000 km. As we saw in (Jopson *et al.*, 1999) RZ is more robust to PMD impairments compared to NRZ. Here we consider only the effect first order PMD. First order PMD impairment introduce only ISI and this is reduced in RZ as pulse width of RZ is lesser compared to NRZ.

CHAPTER 3

POLARIZATION DIVISION MULTIPLEXING SYSTEM

3.1 Overview of PDM system

Polarization Division Multiplexing (PDM) is one of the methods used to double the bit rate with in the available bandwidth where a single fiber can carry two independent optical signals at the same wavelength since they are launched in orthogonal polarization states. A new scheme for coding optical signals using the polarization of light is described by (Herard and Lacourt, 1991). This was the consequence of the vectorial nature of electromagnetic waves and they described experimentally 50 m link for the first time. Then (P.M.Hill *et al.*, 1992) came up with an optical polarization multiplexing system using BPSK coherent heterodyne detection to transmit 4 Gb/s over a 45-km standard single-mode fiber optical link at a receiver sensitivity of -35 dBm. Although it is relatively simple to multiplex two orthogonally polarized optical signals into a single fiber, it is far more difficult to demultiplex the two signals at the end of the optical transmission line because conventional single mode fibers do not maintain the state of polarization (SOP). Although the multiplexed optical signals remain orthogonally polarized in the fibre over distances of more than 100 km, their absolute SOPs at the receiver are generally unknown and even change with time. So for the first time a fully automatic polarization demultiplexer for PDM transmission systems was introduced by (Heismann *et al.*, 1993). Operation of the demultiplexer is demonstrated in a 20 Gbps PDM transmission experiment at a wavelength of 1540 nm, where two 10 Gbps channels are automatically demultiplexed after traversing 134 km of dispersion-shifted fiber. Then people studied the coherent cross talk between the orthogonal polarizations which is the main drawback of this technique. There will be combined effect of PMD and PBS misalignment. The simplified expression for complex amplitude at the output takes the form (Nelson and H.Kogelnik, 2000),

$$A_{out} = A + i\kappa_0 B + (\triangle\tau/2)\,\dot{B} \tag{3.1}$$

Here it is assumed a 45^0 worst case launch into the fiber. $\triangle\tau$ is the Differential Group Delay (DGD), κ_0 is coupling constant generally a complex number whose phase depends on nature of misalignment. A and B denotes the two orthogonal polarization channels and the second term in equation. 3.1 denotes the crosstalk due to the misalignment of the PBSs and the third term in equation. 3.1 denotes the crosstalk due to PMD (Nelson and H.Kogelnik, 2000). Then studies on PDM systems progressed and (Z.Wang *et al.*, 2009) investigated polarization mode dispersion (PMD) and polarization dependent loss (PDL) impairments in polarization division multiplexing (PDM) signals with optical polarization demultiplexing and direct detection. In their work they show that time alignment between the bits in the two polarization has a significant impact on PMD impairments and it also depends on the PDM signal bandwidth where as Polarization Dependent Loss (PDL) is independent of all these factors. This work also shows that by proper configuration of polarization demultiplexing, the PDL induced crosstalk can be completely eliminated. And impairment from one effect (either PMD or PDL) does not enhance that from the other. Then studies were concentrated on combining PDM with higher order modulation formats. Optical transmission characteristics of wavelength-division multiplexed (WDM) and polarization-multiplexed (POLMUX) signals using high-order optical quadrature-amplitude-modulation (QAM) formats was studied in (K.Kikuchi, 2011). The research has gone through PDM-OFDM also other than PDM-WDM systems. In (Wang *et al.*, 2012) experimentally demonstrate a direct-detection polarization division multiplexed (PDM) orthogonal frequency-division multiplexing (OFDM) scheme without dynamic polarization tracking. Recently studies propose a polarization demultiplexing method in Stokes space for coherent optical PDM-OFDM without inserting training symbols (Z.Yu *et al.*, 2013).

In this chapter we describe the simulation of PDM system. We concentrate more on PDM-NRZ and PDM-ODB here, as our experiments were carried in those modulation format. Increased reach of upto 350 km was demonstrated in the past with the use of PDM-ODB format with dispersion compensation and active control of polarization (P.Boffi *et al.*, 2008). We conduct experiment with fiber length up to 100 km. In order to find the extent of the dispersion tolerance of the PDM-ODB system we simulate the performance of the system for longer lengths of the fiber and at the end of the chapter we compare the OSNR penalty to achieve BER of 10^{-9} for different formats.

3.2 Simulation of PDM system

Usually PDM system is used with higher order modulation formats like QPSK, QAM etc. But we are dealing with NRZ and ODB formats in the experiments. So here we simulate PDM-NRZ and PDM-ODB systems. For simulation we used the matlab functions provided in the optilux package. For single polarization systems (ordinary systems) we initially put data only in one of the polarizations of electric field (either $E_x$or E_y). But in PDM systems we put two different data in both E_x and E_y. Then the procedure is same as that of what we did to study the PMD effects. It solves the PMD-Manakov equation. After propagation we need to retrieve the data in two polarization. But the detector does not know (or can't distinguish) between E_x and E_y. So in the receiver side we used a linear polarizer function $polarizer(\theta, \epsilon)$, which has two arguments azimuth angle (θ) and angle of ellipticity (ϵ). We simulated the same scenario as that of two slow axis of PBS (which are perpendicular to each other) by providing 90^0 phase shift between the linear polarizer. In our experiment we got an extra penalty of around 3.5 dB in b2b PDM system. This is mainly because of the lower extinction ratio of the PBS (15 dB only) which is due to the misalignment in the slow axis. So to simulate the same scenario we used some misalignment in the polarizer w.r.t the signal at receiver side.

3.2.1 NRZ and ODB system

Fig. 3.1 shows the simulated results of NRZ systems at 10 Gbps. We simulated for different fiber lengths (25 km to 120 km) and we observe that after 25 km of fiber length the OSNR required to achieve a BER of 10^{-9} increases drastically. This is mainly due to chromatic dispersion limit of the system, as at 10 Gbps PMD impairment at these fiber lengths is found to be negligible (discussed in chapter. 2). More or less the same trend is obtained in our experimental results which will be discussing in chapter. 4.

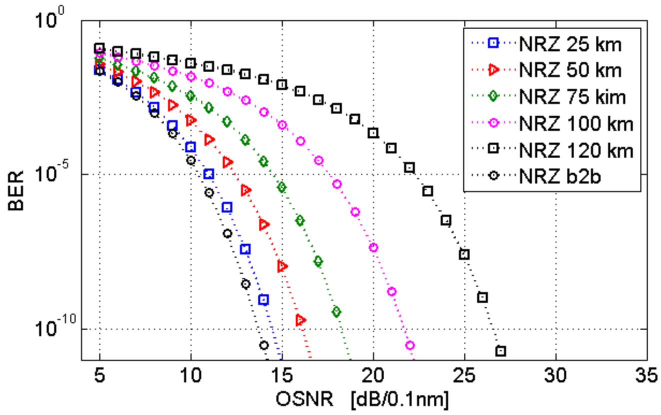

Figure 3.1: BER calculated for different values of OSNR for the NRZ modulation format at 10b Gbps datarate for different lengths of the fiber

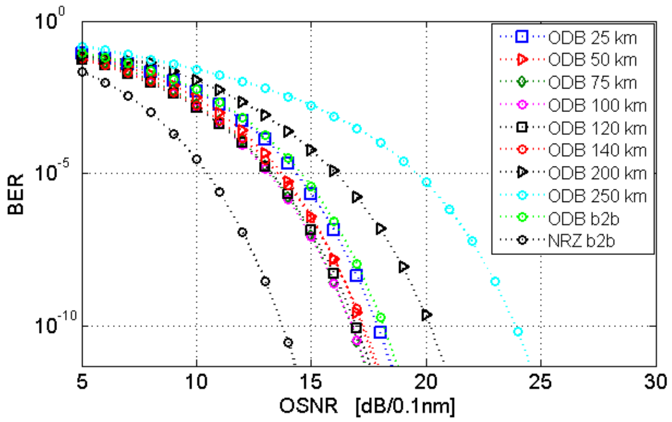

Figure 3.2: BER calculated for different values of OSNR for the ODB modulation format at 10b Gbps datarate for different lengths of the fiber

Fig. 3.2 shows the simulation results of ODB system. We can see the b2b ODB result shows more penalty than b2b NRZ case. But for fiber length more than 50 km the OSNR penalty (at BER of 10^{-9}) is lesser in ODB than that in NRZ. This is because of the chromatic dispersion tolerence of ODB modulation format, which is due to the narrow spectrum of ODB. Carrier also absent in ODB as we bias modulator at its null point (see Fig. 3.3).

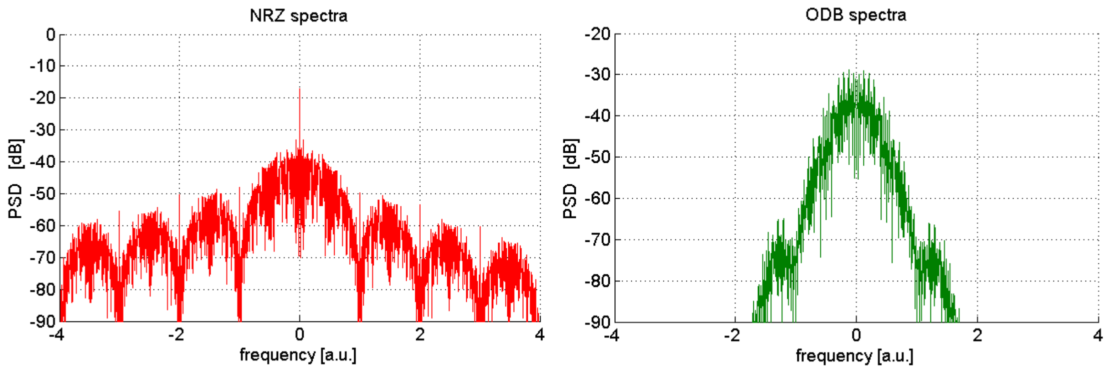

(a) NRZ spectra (b) ODB spectra

Figure 3.3: NRZ and ODB spectra to show the narrow spectra for duobinary

This dispersion tolerance was quite clear in the experimental results also which we discuss in chapter. 4.

3.2.2 PDM-NRZ system

Now we explain the simulation results of PDM systems. As we mentioned in the beginning, here we put two different data in two polarization and multiplexed signal is fed to the fiber. The total power of the combined signal was kept at 0 dBm which is similar to what we used in the experiment. As the SOP will keep on changing along the length of the fiber, at the receiver we changed the Polarizer angle such that always the data quality in the two polarization channel in PDM are equally good. Same thing we do in our experiment where we manually control the polarizer before the receiver such that both port of demultiplexing PBS show same BER for a given OSNR.

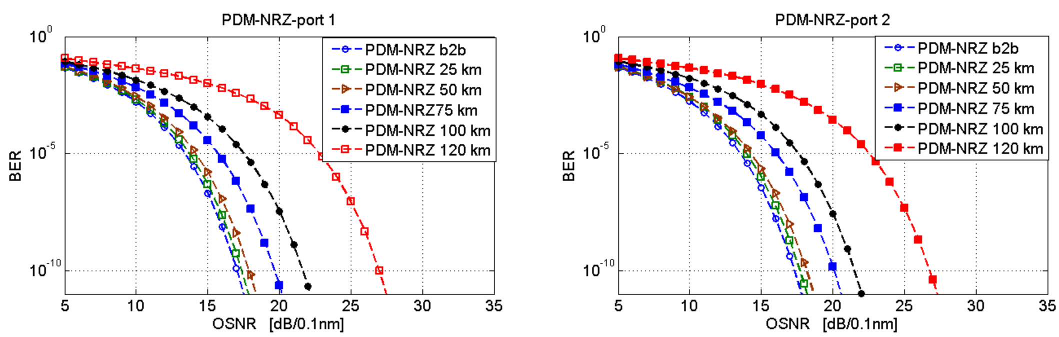

(a) PDM NRZ PBS port1 output (b) PDM NRZ PBS port2 output

Figure 3.4: BER calculated for different values of OSNR for the PDM-NRZ modulation format for different lengths of the fiber observed in two different ports of the PBS

Fig. 3.4 shows the simulation results of PDM-NRZ system. We can see port 1 and port 2 results are more or less the same, i.e; performance-wise both polarization channels are same. The trend of the OSNR penalty with increase in fiber length is same as that of NRZ case (Fig. 3.1). If we do not consider the effect of misalignment of slow axis of PBS, here also we will get exactly the same OSNR penalty as that of NRZ case.

3.2.3 PDM-ODB system

PDM-ODB simulation was also done by keeping all previously mentioned conditions like same performance in both polarization, misalignment of PBS slow axis etc. Fig. 3.5 shows the results of the simulation. Both port 1 and port 2 results are almost same. Here to see the extent of dispersion tolerance we simulated up to a distance of 200 km. Similar to what we saw in Fig. 3.2 the b2b PDM-ODB shows more OSNR penalty than that of b2b PDM-NRZ.

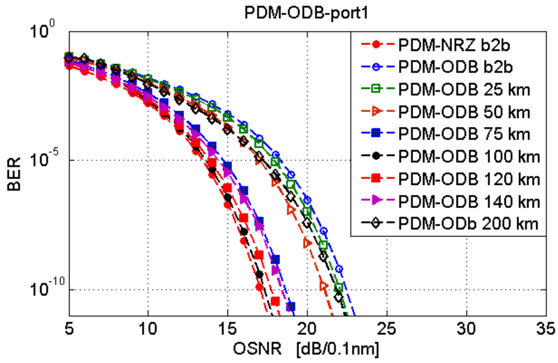

(a) PDM ODB PBS port1 output

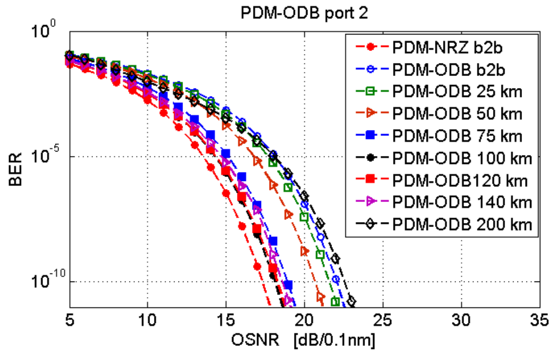

(b) PDM ODB PBS port2 output

Figure 3.5: BER calculated for different values of OSNR for the PDM-ODB modulation format for different lengths of the fiber observed in two different ports of the PBS

At longer length (>50 km) the system shows better performance due to its dispersion resilient nature. Upto 100 km the OSNR penalty was decreasing with increase in fiber length. After which it starts increasing with fiber lengths. But upto 200 km penalty was below that of b2b PDM-ODB case.

3.2.4 OSNR Penalty comparison of NRZ, ODB, PDM-NRZ and PDM-ODB systems through simulation

Fig. 3.6 shows the OSNR penalty comparison of different modulation formats like NRZ, ODB, PDM-NRZ, and PDM-ODB.

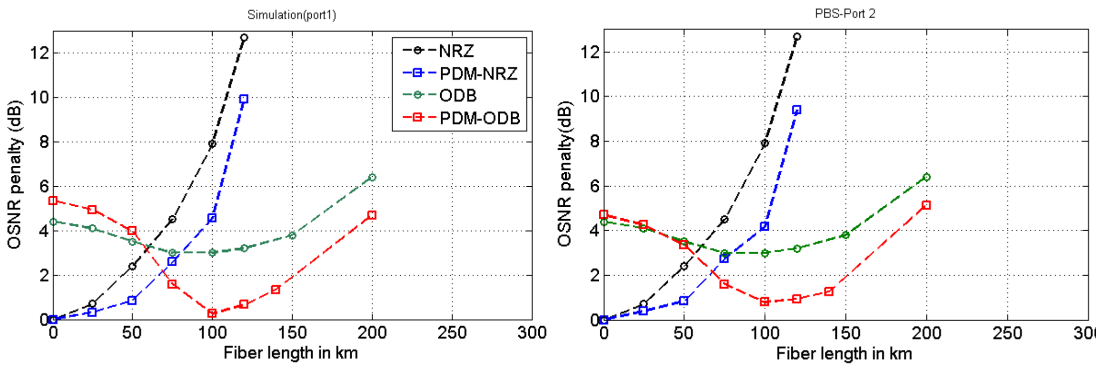

(a) PBS port1 output (b) PBS port2 output

Figure 3.6: OSNR penalty for different modulation formats, calculated as a function of the length of the fiber

Here OSNR penalty is calculated for a BER of 10^{-9}. For NRZ and ODB case the penalty calculation is done w.r.t OSNR value corresponding to b2b NRZ. And for PDM case the OSNR penalty is found w.r.t OSNR value of b2b PDM-NRZ. Fig. 3.6 gives the overall idea of the variation of OSNR penalty with fiber length and the modulation format in both the polarization channels. It is shown that the ODB is having more reach for a given OSNR value. And it is also interesting to note that in PDM-ODB case the penalty is lesser than that of ODB case. We are investigating the reason for this. The same effect we could see in the experimental results as well.

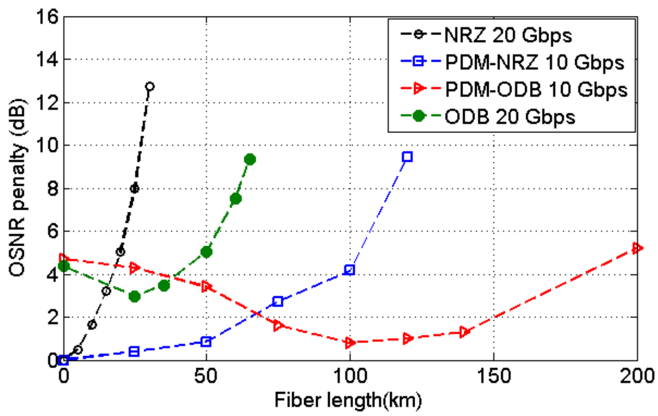

Figure 3.7: OSNR penalty calculated as a function of the length of the fiber, PDM system at 10 Gbps (effective data rate 20 Gbps) and NRZ and ODB at 20 Gbps

Fig. 3.7 shows the importance of PDM system for sending higher data rates. Here we simulated the single polarization channel for NRZ and ODB with 20 Gbps data. OSNR penalty is calculated using b2b NRZ value at 20 Gbps. It is compared with the OSNR penalty of PDM-ODB and PDM-NRZ case. In PDM case as mentioned before, penalty is calculated with respect to b2b PDM-NRZ OSNR value. Even though the data rate in each polarization channel is 10 Gbps, the effective datarate of the PDM signal is 20 Gbps. From Fig. 3.7 it is very clear that at 20 Gbps single polarization case even ODB signal reach is very less. So attaining spectral efficiency using PDM and hence by increasing the datarate is more convincing and promising technique.

CHAPTER 4

EXPERIMENTAL RESULTS OF PDM SYSTEM

In experimental part we want to demonstrate the dual polarization scheme and how it helps to double the bitrate with in the available bandwidth using the single wavelength. As a first step of the experiment we identified the components required and characterized those components. Among those components Polarization beam splitter (PBS) (Fig. 4.1) was the most important one.

4.1 Polarization Beam combiner/Splitter(PBC/PBS)

We used Thorlab's SMF based PBS. It has two legs of polarization maintaining (PM) fiber on one side of calcite prism and a single mode fiber on the other. The legs on the side with the two PM fibers have the slow axis of the fiber aligned for maximum transmission of one polarization state. If an unpolarized signal is sent into the single mode fiber (port 3), the calcite prism splits light into orthogonal linear polarizations. The slow axis of each PM fiber is aligned to each of the polarized beams emitted from the prism (port 1 and 2). Light incident on port 1 and 2 should be aligned to the slow axis. Light incident at port 1 and 2 aligned to the fast axis of the fibers will refract differently through the prism and will not exit port 3. Slow axis of port 1 and port 2 are designed such that they are orthogonal to each other.

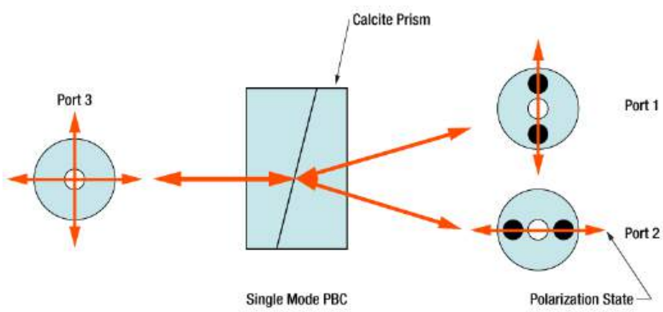

Figure 4.1: Polarization Beam Splitter internal structure (source: Thorlabs)

4.1.1 Insertion loss of Polarization Beam Splitter

To find the insertion loss of the PBS we used the setup as shown in Fig. 4.2. By simultaneously monitoring power from port1 and port2 we can identify the polarization of the source used. We directly gave the input from the SFP module of the PRBS generator (1.65 dBm) into the port 3 of the PBS and tried to control the polarization using the polarization controller. At the maximum we could get only -9.5 dBm in one port and in other port with a maximum extinction ratio of 24 dB (-33.5 dBm). But the maximum insertion loss (as per the given data sheet of the PBS) is 0.7 to 0.8 dB only. But here we are getting higher (more than 10 dB) insertion loss. So we could conclude that PRBS source is only partially polarized. Since PRBS is giving partially polarized light the calcite prism splits light into orthogonal linear polarizations and some of these linear polarizations may not be aligned to any of the two slow axes corresponding to either port 1 or port 2 and hence those will be contributing loss. We did the experiment with the TLS directly instead of PRBS generator and then we got insertion loss of 0.3 dB only as TLS is highly polarized. One more thing we realized is even with the PRBS if we use PBS in the reverse way (i.e., if we give input to the port1 or port 2 and take output at common port (port 3) the insertion loss is lesser (around 7.7 dB).

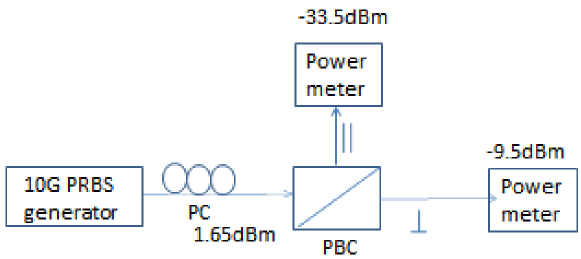

Figure 4.2: Experimental setup to find the insertion loss of the PBS

4.2 Polarization Division Multiplexing experimental setup (without noise loading)

As an initial part of a Polarization Division Multiplexing experiment, we put data only into one of the orthogonal polarization states. This was accomplished by using input to one of the input ports of PBS1 (say port1) and by using the PC the output at port 3 is made maximum. Then to see the cross talk (coherent) in back to back transmission we gave this output to the port 3 of an another PBS2 and observed the power levels at port 1 and port 2. Now as expected we got the maximum power (almost the same power in port 3 of PBS1) in the port 1(of PBS2) and a very little amount of power in the port 2 (due to cross talk). Then we captured the eye from the port1 of PBS2, and we compared the eye that we captured from the port 3 of PBS1.

Here we did not specify any specific data sequence. Our aim was to see Polarization beam combining and polarization beam splitting were working fine, with the single polarization scheme. From the above results (the eye diagrams and the power levels) we could conclude PBSs can be used for polarization division multiplexing and we preceded the experiment to study the transmission quality of a polarization division multiplexed signal using dual polarization scheme as shown in the experimental setup in Fig. 4.4. We used PRBS in user defined sequence (used 10101110 sequence). 50:50 coupler was used to split the power equally (almost) in both channels. Now to decorrelate the data in two channels we used a 5 m SMF (which gives a delay of 25 ns) in one of the channels. By adjusting the PCs these two different data were sent in orthogonal polarizations. VOA was used in the other arm to adjust the power level such that the power levels in both the channels were made almost equal if at all any difference was there. Wave forms and eye diagrams were captured for the different data and the polarization division multiplexed data (PBS1 port3). Then the combined signal was sent to the next PBS (PBS2) which was used to demultiplex the data. As we did in the previous step, we captured waveforms and eye diagram of the demultiplexed data also (in port1& port2 of PBS2). At each stage we noticed the power levels (indicated in the experimental setup) and used the proper attenuation for getting better results.

The PDM data is obtained as shown in Fig. 4.4 (the output of PBS1, port3). We expected 3 levels only (0, 1, 2) after the delayed data are combined. Here we can see the data has not exactly the three levels. This is because of the unequal power levels present in the two data. Even though we try to make the amplitudes equal, due to very small random fluctuations in the polarizations those amplitude won't be exactly equal. Thus we can transmit 20 Gbps data (2×10Gbps) with in the same bandwidth and in the same wavelength.

Finally we could successfully demultiplex the two data from the multiplexed data. The waveforms obtained are as shown in Fig. 4.3 and Fig. 4.4. From the eye of the two data streams (PBS1 port 1& port2) we can see the BER (eye) is very low. The eye diagrams of the two demultiplexed data are shown at PBS2 port1&port2. The BER (eye) is becoming higher (of the order 10^{-4}).

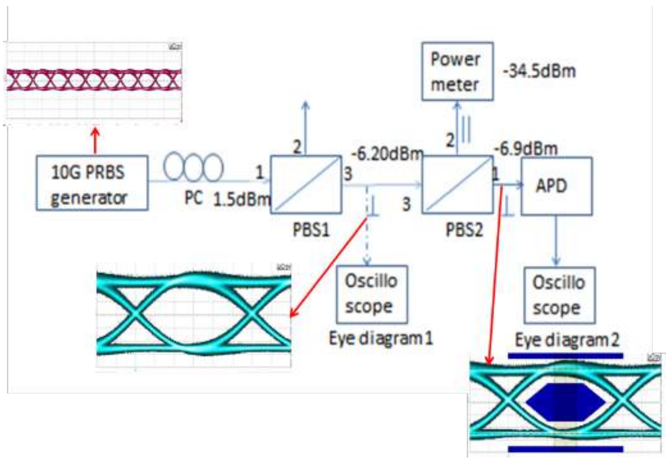

Figure 4.3: Experimental setup with single polarization (without noise loading)

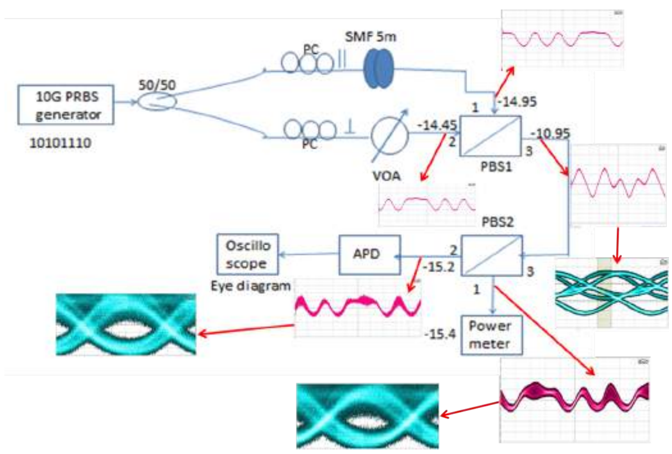

Figure 4.4: Experimental setup for PDM system (without noise loading)

We introduced the noise loading mechanism and then repeated the experiment at different noise level. BERT is used to take the BER vs OSNR for this back to back setup for the PDM signal. To begin with the noise loading part, we first characterized the EDFA.

4.2.1 Noise loading EDFA (home made) characterization

The experimental setup for the EDFA characterization is as shown in Fig. 4.5. The Tunable Band Pass Filter (TBPF) is used to limit the broad band nature of the ASE from the EDFA. We also noted down the OSNR at different received power levels.

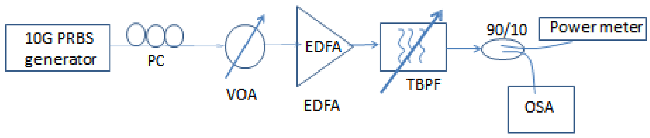

Figure 4.5: Experimental setup for EDFA characterization and OSNR calculation

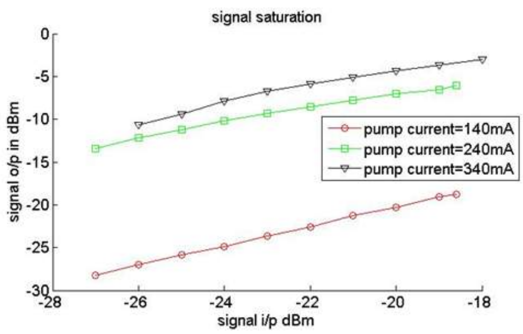

(a) Signal saturation

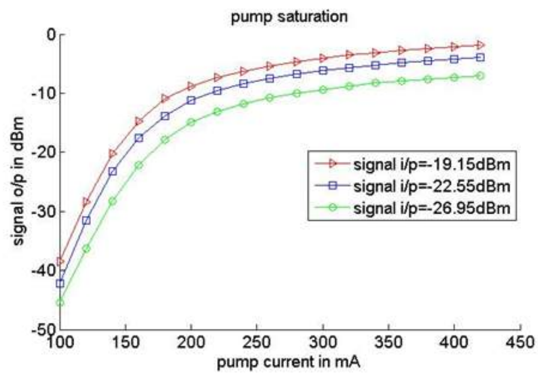

(b) Pump saturation

Figure 4.6: EDFA signal and pump saturation

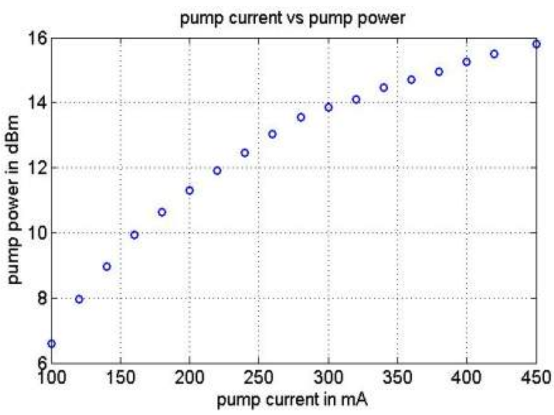

(a) Pump current at different pump power

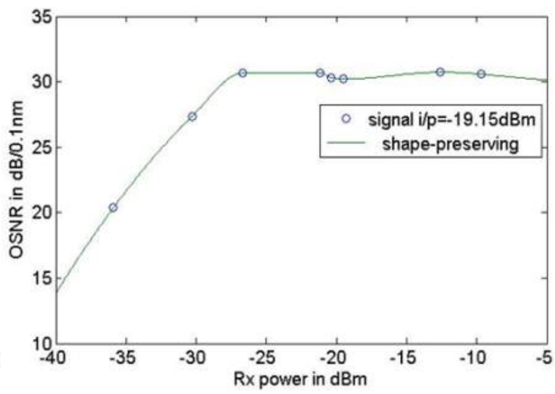

(b) OSNR vs Received power

Figure 4.7: Pump current and OSNR range of EDFA

Fig. 4.6 (a) shows the signal saturation characteristics of EDFA. For signal saturation we kept pump current constant and observed EDFA output for different input power by varying the attenuation in VOA and the signal saturation curve was plotted with output signal power vs. input power. We repeated this experiment for three different pump current (140, 240 and 340 mA). The pump saturation of EDFA is plotted in Fig. 4.6 (b) with pump current (mA) vs.output signal power. Here signal power is kept constant and varied the pump current and noted down the output signal power and repeated the same for three different signal power. In Fig. 4.7 (a) pump current (mA) vs. pump power (dBm) is plotted. This plot gives an idea about pump power corresponding to a pump current and which in turn we can refer to Fig. 4.6 (b). Fig. 4.7 (b) shows OSNR variation we could get from the homemade EDFA. For a particular signal input (-19.15 dBm) varied the pump current and found the OSNR corresponding to each received power and we could find that the EDFA gave a 15 dB (15 dB/0.1 nm to 30 dB/0.1 nm) OSNR variation for received power varied from -40 dBm to -25 dBm.

4.3 Experimental setup for BER vs. OSNR measurements

'BER vs. OSNR' is a generally used performance measure of any communication system. It generally contains three major part: Modulation and transmission, Noise loading, and OSNR and BER measurement at receiver side. Here we are discusing four types of systems.(1) NRZ, (2) Optical Duobinary (ODB), (3) PDM-NRZ and (4) PDM-ODB.

4.3.1 Experimental setup for NRZ/ODB system

The experimental set up for the propagation of data in the ODB format, through a 100 km of standard single mode fiber is shown in Fig. 4.8. Light output from a DFB laser at 1550 nm is modulated using an external Mach-Zehnder modulator biased at its null. It was modulated with $2^7 - 1$ PRBS data at a rate of 10 Gbps derived from BERT (Optellent). The PRBS data is allowed to pass through low pass Bessel filter of bandwidth 2.75 GHz to result in a three level duo-binary signal. The output of the filter is amplified using an RF driver and is fed to the RF port of the modulator.

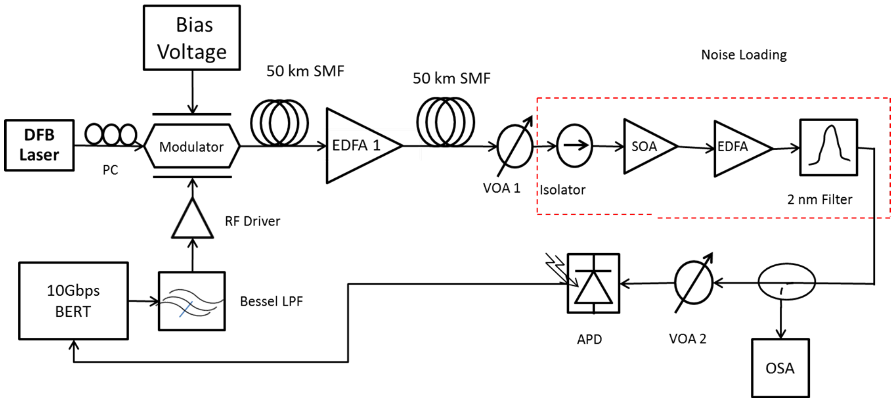

Figure 4.8: Experimental setup for NRZ/ODB system

The 10 Gbps ODB signal thus generated is transmitted over different fiber lengths (50 km, 75 km and 100 km). An EDFA with low noise figure is used to amplify the signal after 50 km fiber length. A noise loading stage consisting of an isolator, semiconductor optical amplifier (SOA) and EDFA is used at the output of the propagation fiber to vary the OSNR at the receiver. Bias current of SOA and pump current of EDFA are changed to obtain the desired noise. We used WDM application of the Optical Spectrum Analyser (OSA) with the resolution bandwidth of signal is fixed at 0.2 nm and that of noise 0.07 nm for the OSNR measurements. We tap 10% of the received power to the OSA and 90% for BER measurement using a 90:10 coupler. Now this signal is fed to a 10 Gbps Avalanche Photo diode (APD) and this detected signal is fed back to the analyzer of the BERT to measure the corresponding BER. The VOA before detector is used to ensure that the power falling on the detector and hence the shot noise contribution does not change with the OSNR. We use the same experimental setup to generate 10 Gbps NRZ by removing Bessel filter and biasing modulator in the linear region of its transfer curve.

4.3.2 Experimental Results and discussion of NRZ and ODB systems

Fig. 4.9 shows the BER vs. OSNR curve for NRZ data in single polarization. At 10 Gbps we know the PMD effect is negligible. So the penalty is mainly due to the chromatic dispersion. And the OSNR penalty is calculated for BER of 10^{-9} , with respect to the b2b NRZ performance. As the fiber length increases the penalty also found to be increased. The experimental results shown in Fig. 4.9 tell that the OSNR requirement for a BER of 10^{-9} at a fiber length of 100 km is very high (around 23 dB/0.1nm). So we can infer that without chromatic dispersion compensation it is difficult to get the long reach if we use NRZ modulation format for transmission. So we tried dispersion resilient ODB formats for longer reach.

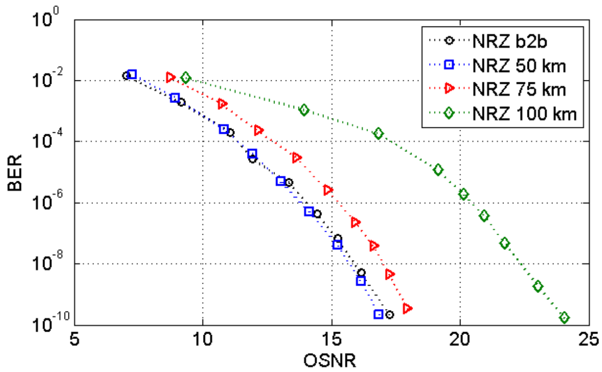

Figure 4.9: Experimental results of NRZ sytems

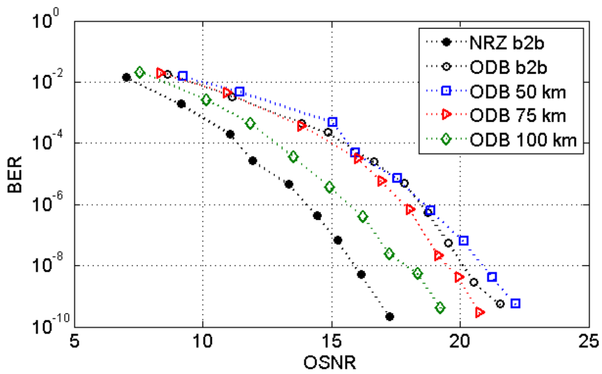

Figure 4.10: Experimental results of ODB sytems

Fig. 4.10 shows the BER performance vs. OSNR for 10 Gbps ODB data in single polarization, measured for different lengths of the fiber. The BER for the NRZ b2b case is also shown for comparison. We observe that the OSNR requirement is larger for ODB b2b compared to that of NRZ. However, it is interesting to note that, the OSNR required to achieve a given BER decreases with the increase in the length of the fiber for the ODB case. This is due to the inherent dispersion tolerance property originating from the narrow spectrum occupied by the ODB signal as discussed earlier. Thus, long-reach PON networks of up to 100 km are possible with the use of ODB modulation format with dispersion resilience.

4.3.3 Experimental setup for PDM-NRZ/PDM-ODB system

The experimental set up for the propagation of data in the PDM-ODB format, through a 100 km of standard single mode fiber is shown in Fig. 4.11.

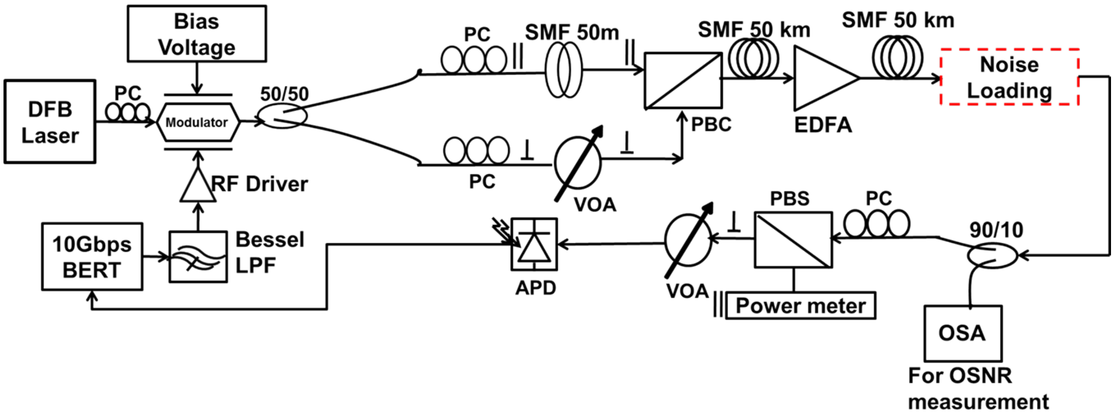

Figure 4.11: Experimental setup for PDM-NRZ/PDM-ODB system

The light is modulated using the same setup explained in Fig. 4.8. The modulated light output is split and the data in the output ports of the splitter is uncorrelated using a 50 m fiber. Two independent and manually controlled Polarization Controllers (PCs) are used to align these two signals into the orthogonal axes of fiber based Polarization Beam Combiner (PBC), thus producing polarization multiplexed optical duobinary/NRZ signal at a data rate of 20 Gbps data rate with 10 Gbps data in each of the orthogonal polarizations. The VOA in one of the channels is used to equalize the power in both the polarizations. The PDM signal thus generated with an average power of 0 dBm is transmitted over different fiber lengths (50 km, 75 km and 100 km).Then the noise loading part is also as same as in the Fig. 4.8. In this setup we measure the OSNR before demultiplexing two orthogonal channels, as we are equalizing the power in the two polarization states. The resolution bandwidth of signal is fixed at 0.2 nm and that of noise 0.07 nm for the OSNR measurements. We use another manually controlled PC and a fiber based Polarization Beam Splitter (PBS) to demultiplex the two orthogonally polarized channels. Now this signal is fed to a 10 Gbps Avalanche Photo diode (APD) and this detected signal is fed back to the analyzer of the BERT to measure the corresponding BER.

4.3.4 Experimental Results and discussion of PDM-NRZ and PDM-ODB systems

Fig. 4.12 shows the variation of BER with OSNR of both the port of demultiplexing PBS (port1&port2) for different lengths of the fiber, in the polarization division multiplexed case, when the modulation is NRZ at 10 Gbps. The Fig. 4.12 also shows the data for a single polarization case, in the back-to- back (b2b) configuration. It is evident that, in the b2b PDM case we see an extra OSNR penalty which is characteristic of the polarization dependent loss of the PBS used in this experiment. This penalty can be reduced drastically with the use of a high extinction ratio PBS (P.Boffi *et al.*, 2008). We adjust the PC manually before the demultiplexing PBS so that rotation in the state of polarization due to fiber propagation can be compensated. As in the case of single polarization, the OSNR required to achieve a given BER increases with the increase in length of the fiber.

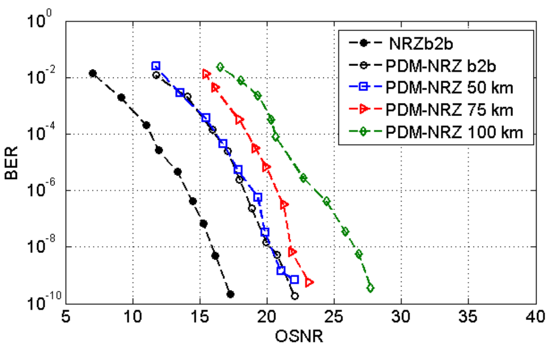

(a) PDM-NRZ o/p at port1

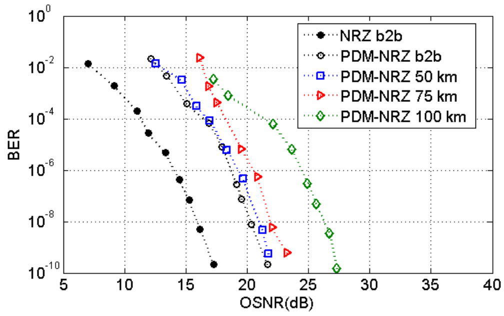

(b) PDM-NRZ o/p at port2

Figure 4.12: Experimental results of PDM-NRZ systems showing output of both port1&port2 of PBS

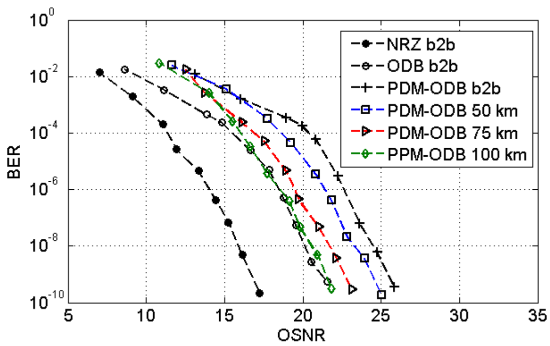

(a) PDM-ODB o/p at port1

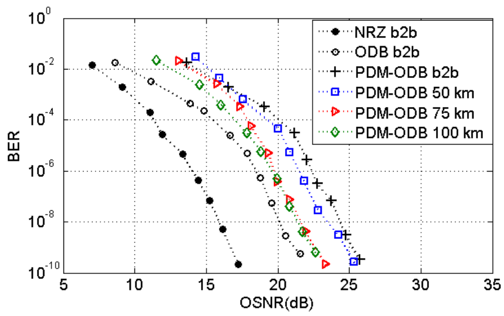

(b) PDM-ODB o/p at port2

Figure 4.13: Experimental results of PDM-ODB systems showing output of both port1& port2 of PBS

We now proceed to demonstrate the possibility of increased spectral efficiency with the use of polarization division multiplexing. ODB data is generated and polarization multiplexed as discussed in the previous section, and Fig. 4.13 shows the experimental results of PDM-ODB system propagated over 50 to 100 km fiber lengths. Fig. 4.13 shows the results obtained at Port1 of PBS and that of Port2. We can see that results are exactly similar to that shown for the single polarization case for ODB modulation. The additional penalty for PDM case seen in Fig. 4.13, compared to the single polarization case is only because of the lower extinction of the PBS used in the experiment.

4.3.5 Experimental set up to investigate the additional penalty present in the PDM system

To investigate the origin of the penalty in the PDM b2b system we removed the data from one of the polarizations (here we removed parallel polarization) and transmitted and received through the PDM set up (i.e; through the two PBS, PCs etc.) and we measured the OSNR after splitting (i.e; after PBS2) as shown in Fig. 4.14.

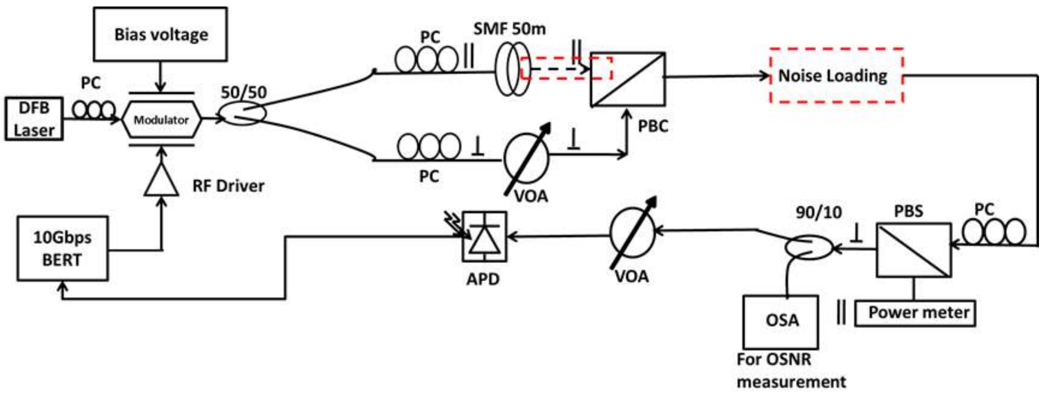

Figure 4.14: experimental set up to investigate the additional penalty present in the PDM system

Fig. 4.15 shows the BER vs. OSNR plot with results of NRZ b2b case, PDM-NRZ b2b case and NRZ b2b case when the single polarized NRZ data passes through two PBSs and PCs (i.e; the polarization dependent components in the PDM setup). This study helps us to observe the extra penalty present in the aforementioned two systems compared to b2b NRZ. From Fig. 4.15, at BER of 10^{-5}, the OSNR penalty is 2 dB in the NRZ b2b with data only in port 2 case, where it is 3.5 dB in the DP-NRZ b2b case. So it clearly shows there is a penalty due to some PDL and PBS misalignment.

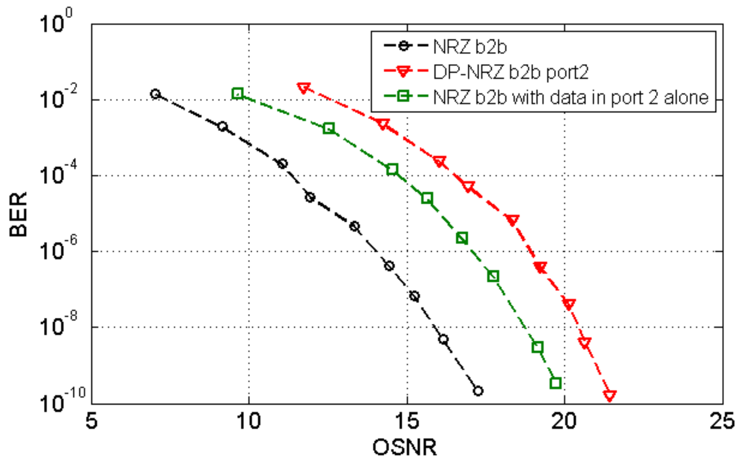

Figure 4.15: Experimental results showing an inherent penalty even with single polarization

4.3.6 OSNR measurement after PBS and before PBS in a PDM system

Fig. 4.16 shows the PDM-NRZ experimental setup. It differ from the initial setup (Fig. 4.11) in the OSNR measurement part, where we did the OSNR measurement before demultiplexing the PDM signal. Here we do OSNR measurement after demultiplexing the signal. We conduct this experiment mainly to confirm two aspects. One is to ensure that by doing the power equalization in both polarization channels, we can do a OSNR measurement before demultiplexing PDM signal. Second is to confirm that the extra penalty in PDM system is not due to some mistake in OSNR measurement.

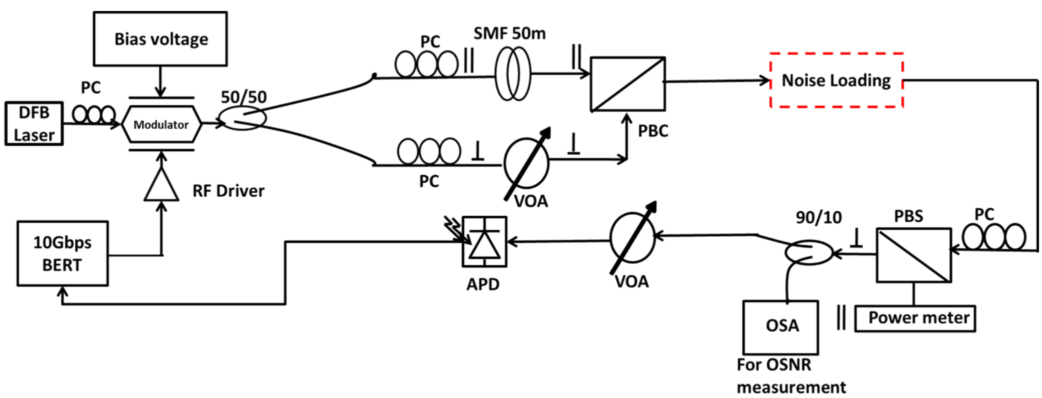

Figure 4.16: Experimental setup showing OSNR measured after the denultiplexing PBS in PDM system

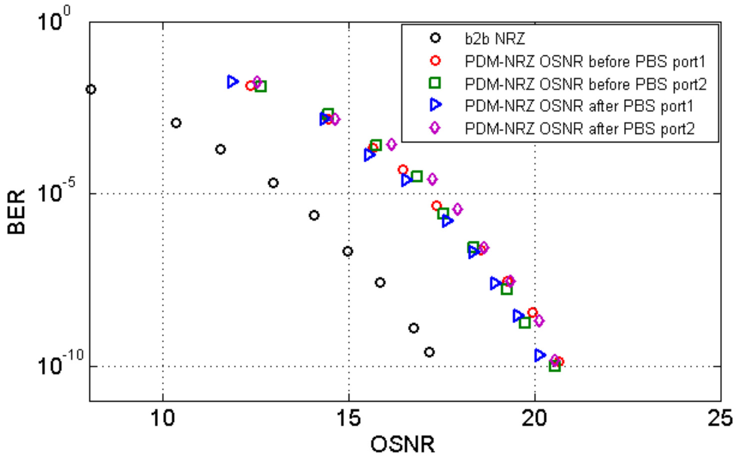

Figure 4.17: BER vs OSNR when OSNR measured before and after the PBS

Fig. 4.17 shows BER vs. OSNR plot obtained from this experiment. It gives detail about two polarization channel present in two port of the PBS and it also compare the results with that we obtained from the initial setup (Fig. 4.11). We can see both Port 1 and Port 2 plots are falling on one over the other. This ensure that the data in both polarization are equally preserved and their performance are similar which also due to the power equalization in two polarization. This results also show that the OSNR measurement in PDM system can be done before or after demultiplexing if we are doing power equalization in both the channels.

4.3.7 OSNR penalty comparison of NRZ, ODB, PDM-NRZ and PDM-ODB systems from the experimental results

OSNR penalty is the key word used to compare the performance of different modulation formats. The penalty plot is shown in Fig. 4.18. It shows the OSNR penalty for different lengths of fiber, with the penalty calculated to obtain BER of 10^{-9}. Here penalty of single polarization is calculated with respect to the back to back (b2b) NRZ at 10 Gbps and that of PDM, with respect to the b2b case corresponding to PDM-NRZ. It is evident that the OSNR penalty in the case of PDM-ODB format is significantly smaller than 7 dB, corresponding to a 10 Gbps NRZ case. It is instructive to note that, the improvement in OSNR penalty in the PDM-ODB case is observable only in the presence of dispersion in the fiber. It is also noted that the penalty for the PDM-ODB case is smaller than the corresponding number for single-polarization case, which is currently investigated.

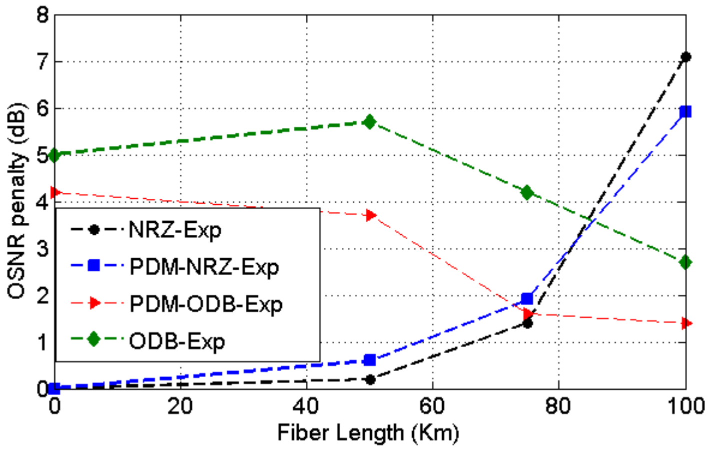

Figure 4.18: OSNR penalty comparison from experimental results

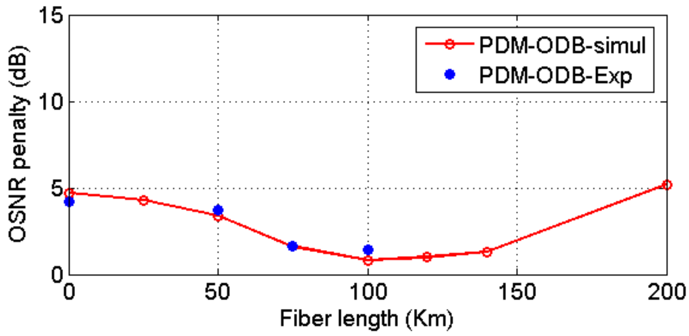

Figure 4.19: OSNR penalty for PDM-ODB data estimated through simulations and Experiments

We have explained the simulation results of PDM system in Chapter. 3. Fig. 4.19 shows both simulation and experimental results together for confirmation of the results. As we mentioned, in order to find the extent of the dispersion tolerance of the proposed PDM-ODB system, we simulate the performance of the system for longer lengths of the fiber. Fig. 4.19 shows the OSNR penalty for different lengths of the fiber, for achieving a BER of 10^{-9}. As the experimental results up to 100 km follows the PDM-ODB simulation results we can expect that the achievable penalty in the experiments for longer lengths of the fiber would be similar to that in the simulations. Thus an extended reach of >100 km with dispersion resilience and increased spectral efficiency is demonstrated with a format conversion from NRZ to PDM-ODB format.

CHAPTER 5

SBS THRESHOLD OF PDM SYSTEMS

5.1 Introduction

Stimulated Brillouin scattering (SBS) limits the optical power that can be transmitted through a single mode fiber in long distance optical communication systems. SBS gain and threshold characteristics of different modulated light was first carried out in (Aoki *et al.*, 1988). It describes higher SBS threshold in modulated light than CW. Dependence of SBS threshold on the laser linewidth and modulation was experimentally confirmed by (Fishman and Nagel, 1993). They showed that broadening the laser linewidth reduces the system degradation from SBS. The polarization dependence of SBS in single mode fibers was studied in (Deventer and A.Boot, 1994). They explained that probe mode with its polarization orthogonal to the pump experiences a brillouin gain half (in dB) of the probe mode with its polarization identical to the pump. Then Dispersion tolerant Optical duobinary transmission system was introduced to get higher SBS threshold as its optical signal has no carrier frequency component (K.Yonenaga and Kuwano, 1997). But for the first time it is shown experimentally that the data coded signal can get higher SBS threshold by employing duobinary modulation format in (T.Franck *et al.*, 1997). It describes very interesting aspects of SBS threshold with respect to modulation formats. The paper investigated the dependency of threshold versus PRBS word length. For NRZ, as the carrier power is dominant and magnitude of carrier is independent of PRBS length no dependency can be seen. But for ODB, SBS threshold is significantly lower for short word length compared to longer word length. Then (E.S.Hu *et al.*, 2004) introduces polarization modulation to increase the SBS threshold due to absence of SPM. Here we are interested in the SBS threshold of NRZ, ODB ,PDM-NRZ and PDM-ODB systems. We do theoretical calculation of SBS threshold and then compare the value with that of the experimental results.

5.2 Theoretical calculation of SBS threshold

One criterion for determining at what point SBS becomes a limiting factor, is to consider the SBS threshold power, P_{SBS}. This is defined as the signal power at which the backscattered light equals the fiber input power. Here we calculate theoretically (a) SBS threshold for CW siganal, (b) SBS threshold for NRZ case, (c) SBS threshold for ODB case.

5.2.1 SBS threshold for CW

The SBS threshold for CW pump light, assuming Lorentzian linewidth profiles, is approximated by (Aoki *et al.*, 1988):

$$P_{SBS}^{CW} \simeq 21 \frac{A_{eff} \times K_{SBS}}{g_B L_{eff}} . \left(\frac{\triangle\nu_{SBS} + \triangle\nu_P}{\triangle\nu_{SBS}} \right) \tag{5.1}$$

where $\triangle\nu_{SBS}$ is the spontaneous Brillouin bandwidth, $\triangle\nu_P$ is the pump light bandwidth, A_{eff} is the effective cross sectional area of the propagating wave, k_{SBS} is the polarization factor, varying between 1 and 2 depending on the relative polarizations of the pump and Stokes waves, and L_{eff} is the effective interaction length given by:

$$L_{eff} = \frac{1 - e^{-\alpha L}}{\alpha} \tag{5.2}$$

where α in m^{-1}. For our calculation we used standared values,
A_{eff}=52.8× 10^{-12} m^2, K_{SBS}=2,Brillouin gain g_B=4.6× 10^{-11} m/W, $\triangle\nu_p$=5 MHz, $\triangle\nu_{SBS}$=20MHz
For L=50 km and α=0.2dB/km, L_{eff}=19.6 km, then $\mathbf{P_{SBS}^{CW}}$**= 3 mW =4.77 dBm**.

5.2.2 SBS threshold for NRZ

The SBS threshold for NRZ is given by (Fishman and Nagel, 1993),

$$P_{SBS}^{NRZ} = \frac{p_{SBS}^{CW}}{1 - \frac{B}{2\triangle\nu_{SBS}}\left(1 - e^{\frac{-\triangle\nu_{SBS}}{f_0}}\right)} \tag{5.3}$$

For 10 Gbps NRZ, B=10 Gbps and f_0=10 GHz and substituting the P_{SBS}^{CW} we get, $\mathbf{P_{SBS}^{NRZ}}$**= 5.99 mW =7.77 dBm**.

5.2.3 SBS threshold for ODB case

For ODB case there is no direct equation as such to calculate the SBS threshold. But logically we know that the threshold will be much higher as carrier is absent in ODB. But to get an approximate number we use the same equation as that of NRZ. We need to substitute half of the bandwidth for ODB compared to NRZ (i.e; for 10 Gbps we take f_0=5 GHz). If we use the equation. 5.3 for ODB and substitute f_0= 5 GHz , we get $\mathbf{P_{SBS}^{ODB}}$**= 1.5 W =31.7 dBm**

5.3 Experiment

The Experimental setup for NRZ/ODB is shown in Fig. 5.1. We calibrated the insertion loss of VOA, circulator and included in the power calculation at each stage (for reflected power, transmitted power and input power). The modulated signal is given as the input to the high power EDFA. The amplified signal is then fed to port 1 of the circulator via a variable optical attenuator (VOA). Port 2 of the circulator is then connected to 50 km fiber spool. Angle connector is used at the end of the fiber to minimize the back reflection. In port 3 of the circulator the reflected power was monitored using a hand held power meter. By varying the attenuation of the VOA different optical power, starting from minimum to maximum, is fed to the fiber and noted down the reading (both o/p and reflected power) at each time. Fig. 5.2 shows the setup for SBS threshold measurement of PDM-NRZ/PDM-ODB case. Here we generate a PDM signal (either PDM-NRZ or PDM-ODB) and it is given to input of EDFA. The remaining experimental setup is similar to what we discussed in Fig.5.1.

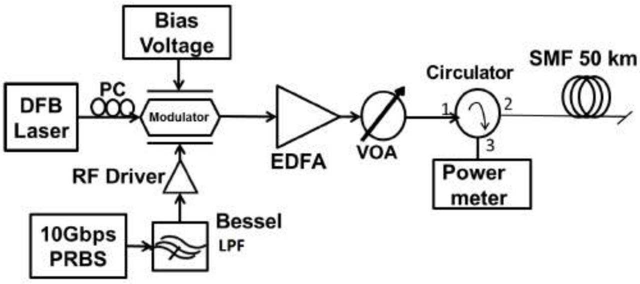

Figure 5.1: Experimental setup for finding SBS threshold of ODB

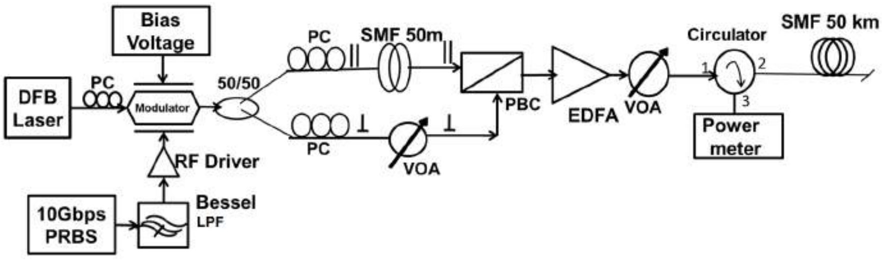

Figure 5.2: Experimental setup for finding SBS threshold of PDM-ODB

5.3.1 Experimental results

Experimental results showing the SBS threshold is shown in Fig. 5.3. We plot reflected power(dBm) in y axis and input power(dBm) in x axis. Here the steeper slope of the curve is extended to touch the x axis to find the SBS threshold.

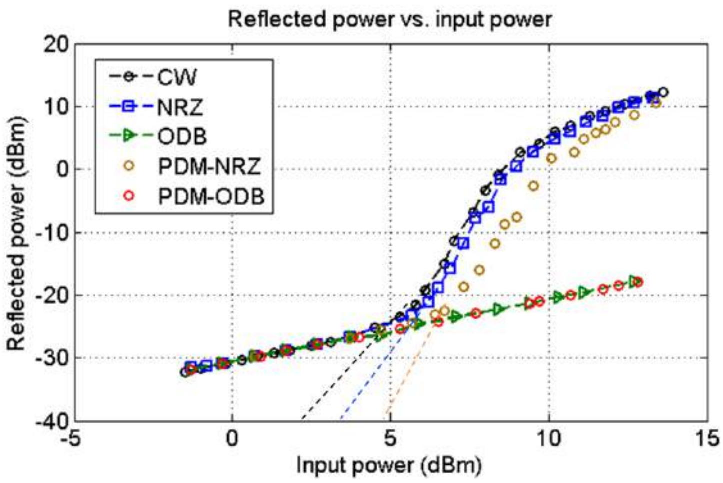

Figure 5.3: SBS threshold for CW,NRZ,ODB,PDM-NRZ,and PDM-ODB case

If we define the SBS threshold as the input power level at which there is sudden increase in the refleced power, and hence the threshold is obtained by extending the steeper slope of each curve to the x axis. From the Fig. 5.3, P_{SBS}^{CW}=2.9 dBm, P_{SBS}^{NRZ}=3.5 dBm, and $P_{SBS}^{PDM-NRZ}$=4.1dBm. The ODB (both SP and PDM case) SBS threshold is pretty high as we expected and we were not able to get the threshold with in an input power level of 15 dBm.

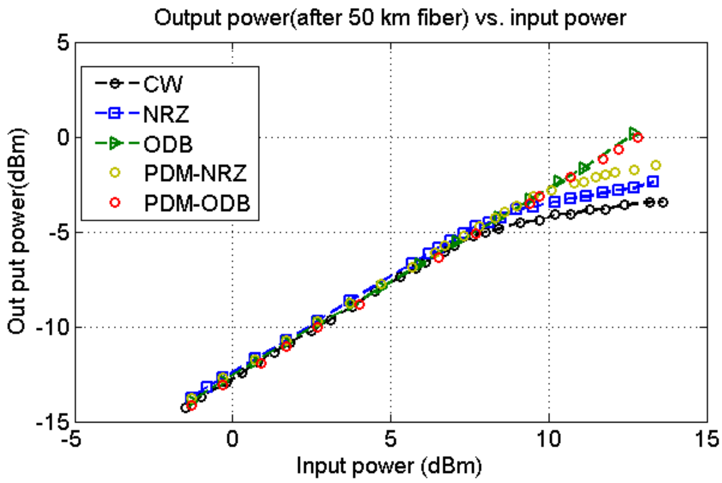

Figure 5.4: Output power at the end of 50 km fiber for CW,NRZ,ODB,PDM-NRZ,and PDM-ODB case

The output power vs. input power plot obtained is shown in Fig. 5.4. One interesting thing we can notice from the experimental result is that, the PDM-NRZ case the SBS threshold is higher than NRZ. We did not get the threshold point in ODB case, but we can expect the same trend in the threshold point for the PDM-ODB case also (that is threshold should be higher for PDM-ODB than ODB). It is well known that SBS is polarization sensitive. When we have had two specific polarizations launched into the system, then the interaction with acoustic waves is effectively reduced, so the threshold is expected to go higher. This may be the reason for the higher threshold for PDM systems.

CHAPTER 6

CONCLUSION

6.1 Summary of the work done

We have done simulation to study the impairment due to PMD in high speed communication system. We carried out simulation with different modulation formats and compared the PMD tolerance. The bitrate dependence of PMD impairment also studied. The maximum reach of the system when PMD impairment alone is considered, for different bitrate also conducted.

We have studied about the Polarization division multiplexing techniques and conducted simulation to understand its performance in NRZ and ODB modulation formats. We conducted experiments to demonstrate PDM-NRZ and PDM-ODB systems and validated the results with the simulation results. Also conducted experiments to study the SBS threshold of PDM-NRZ and PD-ODB system and observed higher SBS threshold for PDM-ODB format.

We demonstrate the utility of the PDM-ODB system for access networks with effective data rate of 20 Gbps with dispersion resilience and higher SBS threshold. The OSNR penalty for propagation through 100 km length of fiber is only 1.5 dB compared to back to back case. So we propose a simple but effective system without changing any active elements in the system level design with minimum cost consisting of optical passive components like Polarization Beam Splitters and Polarization Controllers. Polarization Mode Dispersion (PMD) and its compensation is not a concern in these experiments since the lengths of the fiber used and the bitrate are not sufficient to invoke them. The format converter from NRZ to ODB is a Bessel filter, which can be used as a "plug and play" device for those link that require longer reach. Thus the proposed format conversion is energy efficient as compared to advanced modulation formats and OFDM.

6.2 Scope for future work

Simulation to study the PMD effect can be extended to higher order modulation formats like DQPSK,QAM etc. In our experiment Polarization multiplexing and demultiplexing is performed using passive elements; the possible polarization rotation in the fiber can be countered with the use of electrically controlled polarization controllers with a feedback. Study should be conducted to understand the interesting physics behind the lesser OSNR penalty of PDM-ODB compared to ODB. The SBS threshold experiment can be conducted with different PRBS word length and can see the difference in the threshold with different word length in PDM-ODB system.

APPENDIX A

Algorithm used for simulating the PMD in optical fiber

A.1 Algorithm for simulating PMD

There are two equations to model the PMD in optical fiber. One is Coupled nonlinear Schrodinger equation (equation. 2.1) and another is Manakov equation (equation. 2.2). It uses the Split Step Fourier Transform [SSFM] method in vector form to solve these equations. The basic idea is to resolve the field in to two orthogonal components propagating through the fast and slow axis of the fiber. The algorithm follows the following steps;

A.1.1 Step1: First check which equation (CNLSE or Manakov) is to be solved

In this step we have option to select the equation we want to solve. It can be either CNLSE or Manakov (see equation. 2.1 and equation. 2.2). We choose PMD Manakov equation as it is computaionally simple.

A.1.2 Step2: Calculate the Propagating step size (dZ)

The step size is chosen to have maximum nonlinear phase rotation (ϕ_{max} , which we can define in the simulation). This method of calculating the step size will allow, short steps in region of higher power (usually at the beginning of the fiber) and large steps in regions of low power (usually at the end of the fiber).
Largest normalized power =$max\left(\mid A_x \mid^2 + \mid A_y \mid^2\right)$
Non linear coefficient is γ (1/mW/km) and the attenuation constant is α (1/m).
Effective length of the step can be calculated as, $L_{eff} = \frac{\phi_{max}}{normalizedmaximumpower \times \gamma}$

The propagating step size (dZ) can vary from L_{eff} to the maximum step size that we define in the simulation based on the power, γ and α.

A.1.3 Step3: If the total propagating distance calculated is less than fiber length proceed to step 4 else to step 7

Every time the code updates the propagated distance and if it is less than fiber length go the step 4 which calls the function that deals with the non linearity in the fiber else go to step 7.

A.1.4 Step4: Call the function which deals with non-linearity of the fiber. Here x and y components of Electric fields are propagated through purely nonlinear fiber having nonlinearity and attenuation

This function is to solve either CNLSE or Manakov equation. Here we are dealing only with the Manakov equation. So the effect of nonlinearity on the field components is calculated as follows,

$$power = \left(\mid A_x \mid^2 + \mid A_y \mid^2\right),$$

$$l_{eff} = dZ \; if \alpha = 0,$$

$$l_{eff} = \frac{1 - exp\left(-\alpha.dZ\right)}{\alpha} \; if \alpha \neq 0$$

then fields are calculated as,

$$A_x = exp\left(-i\gamma.l_{eff}.U\right) A_x$$

$$A_y = exp\left(-i\gamma.l_{eff}.U\right) A_y$$

A.1.5 Step5: Call the function which is used to calculate the Birefringence step

Call the function which is used to calculate the Birefringence step and how many such steps are there with in propagating step size (dZ). Throughout the Birefringence step the birefringence is constant and the section will be like a PMF(polarization Maintaining Fiber). So one Wave plate (length equal to propagating step size) will contain many such randomly oriented PMF each of which can be called as the trunks.

A.1.6 Step6: Call the function which applies the linear vectorial step including birefringence and PMD to all the trunks within the same wave plates

First we will take the FFT of x and y electric fields. Then calculate the matrix R, making use of the Pauli$'$s matrix, azimuth angle θ , and the angle of ellipticity ϵ, which describes the change in the basis (the set of linearly independent vectors) over Principal State of Polarizations (PSPs) as follows,

$$\begin{aligned} R\left(\theta\right) &= cos\theta \times \sigma_0 - i.sin\theta \times \sigma_3 \\ &= \begin{bmatrix} cos\theta & -sin\theta \\ sin\theta & cos\theta \end{bmatrix} \end{aligned} \tag{A.1}$$

$$\begin{aligned} R\left(\epsilon\right) &= cos\epsilon \times \sigma_0 + i.sin\epsilon \times \sigma_2 \\ &= \begin{bmatrix} cos\epsilon & i.sin\epsilon \\ i.sin\epsilon & cos\epsilon \end{bmatrix} \end{aligned} \tag{A.2}$$

$$R = R\left(\theta\right) \times R\left(\epsilon\right) \tag{A.3}$$

Now we calculate a diagonal matrix D which contains birefringence, DGD and GVD; GVD parameters are the derivatives of order greater than 1 of $\beta\left(\omega\right)$ at $\omega = \omega_0$. Usually only β_2 and β_3 are included inthe NLSE, and hence the NLSE becomes:

$$\frac{\delta A}{\delta z} = -\beta_1 \frac{\delta A}{\delta t} + j\frac{\beta_2}{2}\frac{\delta^2 A}{\delta t^2} + \frac{\beta_3}{6}\frac{\delta^3 A}{\delta t^3} \tag{A.4}$$

In the frequency domain equation. A.4 can be written as (Agrawal, 2008) and (Serena, 2009),

$$\frac{\delta \tilde{A}}{\delta z} = -j\left(\beta_1\omega + \frac{\beta_2}{2}\omega^2 + \frac{\beta_3}{6}\omega^3\right)\tilde{A} \tag{A.5}$$

The solution of equation. A.5 is,

$$\tilde{A}\left(z,\omega\right) = \tilde{A}\left(0,\omega\right)\exp\left(\beta_1\omega + \frac{\beta_2}{2}\omega^2 + \frac{\beta_3}{6}\omega^3\right)z \tag{A.6}$$

where, $\beta_i = \frac{d^k\beta_i}{d\omega^i} \mid_{\omega=\omega_0}$

For energy conservation principle the energy carried by frequency ω must remain unalterd, i.e;

$$\mid \tilde{A}\left(z,w\right)\mid^2 = \mid \tilde{A}\left(0,w\right)\mid^2 \tag{A.7}$$

Hence GVD parameters include only a pure phase roatation. Now we calculate the diagonal matrix which include DGD, GVD and birefringence effect in it.

$$D = \begin{bmatrix} \exp\left(-i\left(\beta + \triangle\beta\right)L\right) & 0 \\ 0 & \exp\left(-i\left(\beta - \triangle\beta\right)L\right) \end{bmatrix} \tag{A.8}$$

$$\beta = \left(\beta_1\omega + \frac{\beta_2}{2}\omega^2 + \frac{\beta_3}{6}\omega^3\right) \tag{A.9}$$

$$\triangle\beta = 0.5 \times \left(\triangle\beta_0 + \triangle\beta_1\left(\omega\right)\right) \tag{A.10}$$

$\triangle\beta_0$ is the frequency independent birefringence,

$\triangle\beta_1$ is the differential phase shift induced by the PMD; $\triangle\beta_1 = DGD_{rms} \times \omega$,

$DGD_{rms} = \frac{DGD}{numberofwaveplates \times symbolrate}$; first order PMD,

$DGD_{rms} = \frac{\sqrt{\frac{3\pi}{8}} \times DGD}{\sqrt{numberofwaveplates \times symbolrate}}$; higher order PMD.

Now we use the basic linear algebra for change of basis (similarity transformation) and $\left(RDR'\right)\left[A_xA_y\right]^T$ gives the resultant electric field vectors. Finally we take the IFFT of calculated x and y electric fields. The calculation of the Matrix R and the following electric field calculations will be carried out for all the trunks within the same wave plates. So this function is used to model the fiber as the concatenation of PMFs with PSPs randomly oriented.

Again go to step2 to calculate next propagating size.

A.1.7 Step7: Find the last Step size

The last step size means the length of the last wave plate constituting the length of the fiber. And again repeat the same steps from 3 to 6 and at last we will get the x and y components of electric field after propagating through entire length of the fiber.

APPENDIX B

Duobinary modulation format

B.1 Duobinary Modulation

Duobinary modulation is a scheme for transmitting R bits/sec using less than R/2 Hz of bandwidth. By Nyquist's criteria, in order to send R bits/sec with no ISI, the minimum bandwidth required of the transmitted pulse is R/2 Hz. This implies that duobinary pulses will have ISI, but this ISI is introduced in a specific way so that it can be subtracted out to recover the original pulses.

B.1.1 Duobinary encoder

Duobinary signal can be implemented by digitally filtering the data bits with two tap finite impulse response (FIR) filter with equal weights and then low pass filter the resulting signal as shown in Fig. B.1 (H.Shankar, 2002). FIR filter and low pass filter can be combined to a single analog filter of appropriate bandwidth (10 Gbps data stream need 2.8 GHz Bessel filter). This duobinary signal is a three level signal. Since the FIR filter output is correlated signal, all possible sequence of the three value cannot occur. For example output of FIR filter will not contain 1 followed by -1 or vice-versa, and 1 and -1 will always have a zero between them (H.Shankar, 2002). This is one of the reasons for its resilient nature to dispersion.

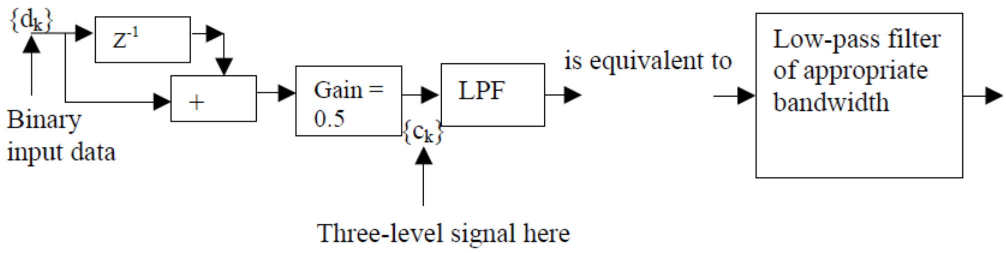

Figure B.1: Differential encoder for ODB [source: (H.Shankar, 2002)]

B.1.2 Duobinary in optical system

Light has to be modulated with three level duobinary signal which gives three level optical signal. This is done with Mach-Zehnder (MZ) modulator biased at null point and with a driving voltage signal swing of $2V_\pi$ volts. The complete duobinary modulator setup is shown in Fig. B.2.

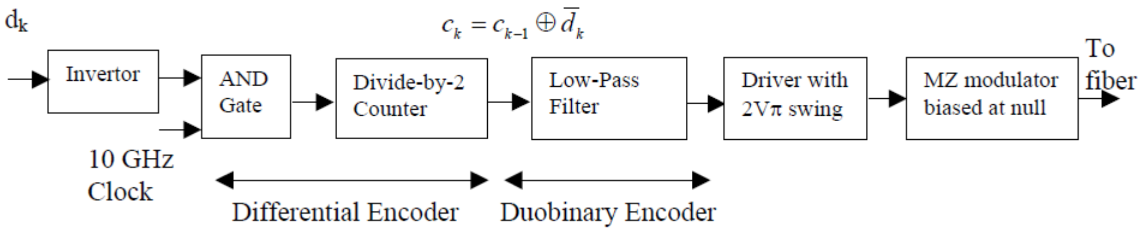

Figure B.2: A Complete ODB modulator [source: (H.Shankar, 2002)]

With zero input, no light is transmitted, but +1 is transmitted as $+E$ and -1 as $-E$. It becomes two level signal in terms of optical power. The Fig. B.3 shows the reason for better dispersion tolerance of ODB compared to NRZ (H.Shankar, 2002).

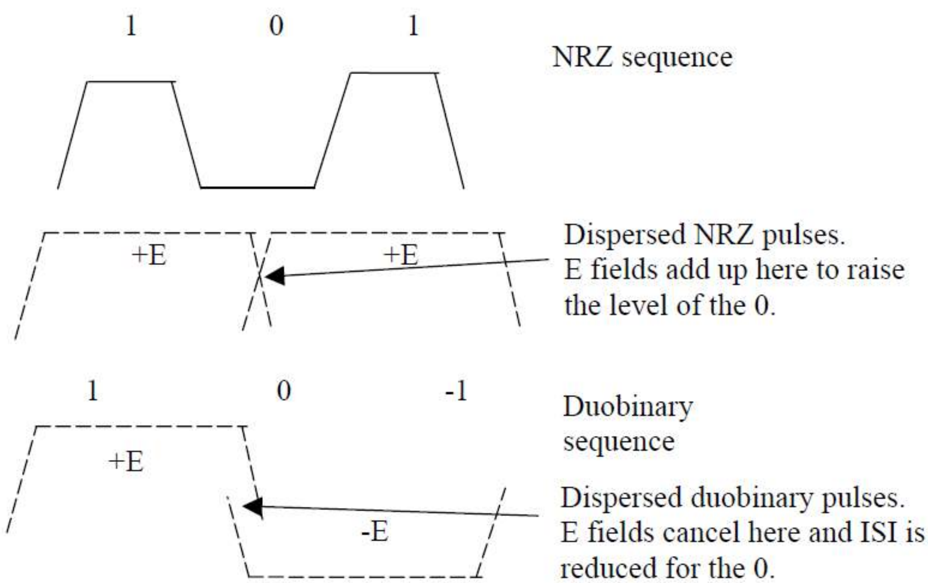

Figure B.3: Effect of dispersion on NRZ and ODB [source: (H.Shankar, 2002)]

APPENDIX C

Experimental set up

C.1 Photograph of basic setup

Basic experimental set up is shown in Fig. C.1 and Fig. C.2. The components are numbered as shown.

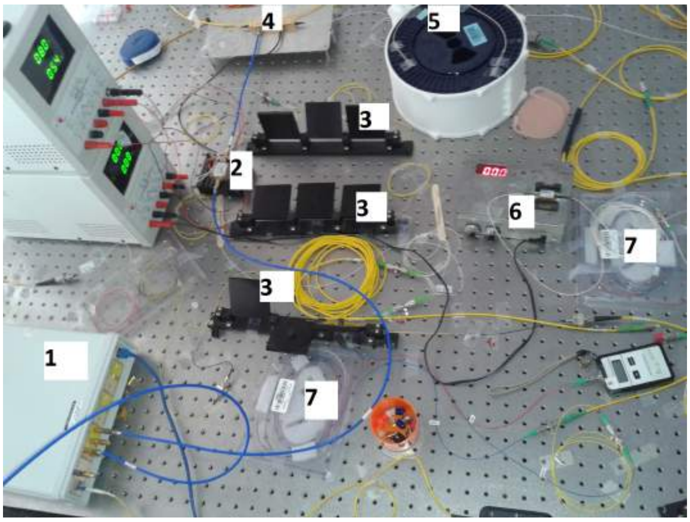

Figure C.1: components in Polarization division Multiplexing (NRZ/ODB) experimental setup

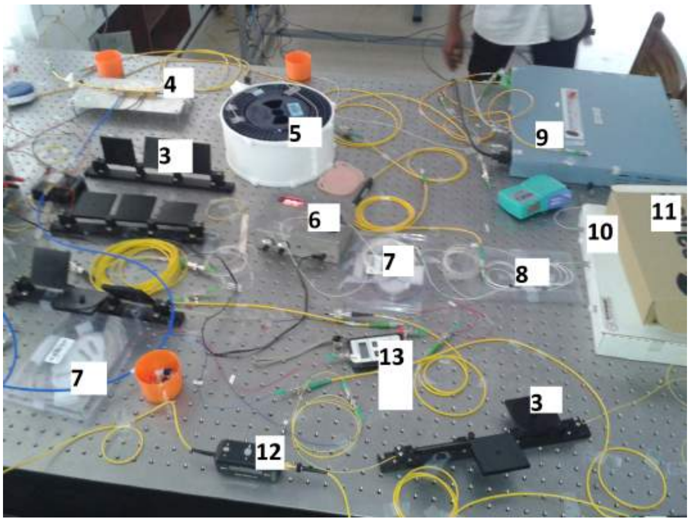

Figure C.2: components in Polarization division Multiplexing (NRZ/ODB) experimental setup

1. Optellent 10 Gbps BERT
2. RF driver
3. Polarization Controllers
4. MZ modulator
5. Fiber spool
6. SOA
7. PBS/PBC
8. Isolator
9. High power EDFA (optiwave)
10. Home made EDFA with high noise figure
11. TBPF
12. VOA
13. power meter

REFERENCES

1. **Agrawal, G. P.**, *Nonlinear fiber optics*. Academic Press, 2008.

2. **A.L.Yi**, **L. Yen**, **B. Luo**, **W.Pan**, and **J.Ye** (2011). All optical signal regeneration in polarization division multiplexing systems. *IEEE Photonics Technology Letters*, **3**(4), 703–712.

3. **Aoki, Y.**, **K. Tajima**, and **I. Mito** (1988). Input power limits of single-mode optical fibers due to stimulated brillouin scattering in optical communication systems. *J. Lightwave Technol.*, **6**(5), 710–719.

4. **C.Xie**, **L.Moller**, **H.Haunstein**, and **S.Hunsche** (2003). Comparison of system tolerance to polarization-mode dispersion between different modulation formats. *IEEE Photonics Technology Letters*, **15**(8), 1168–1170.

5. **Deventer, M.** and **A.Boot** (1994). Polarization properties of stimulated brillouin scattering in single-mode fibers. *J. Lightwave Technol.*, **12**(4), 585–590.

6. **D.Lavery**, **R.Maher**, **D.S.Millar**, **B.C.Thomas**, **P.Bayvel**, and **S.J.Savory** (2013). Digital coherent receivers for long-reach optical access networks. *J. Lightwave Technol.*, **31**(4), 609–620.

7. **D.P.Shea** and **J.E.Mitchell** (2007). A 10-gb/s 1024-way-split 100-km long-reach optical-access network. *J. Lightwave Technol.*, **25**(3), 685–693.

8. **E.S.Hu**, **G. Kalogerakis**, **M.E.Marhic**, **Kazovsky**, and **G.Leonid**, Sbs and nonlinearities reduction of analog optical links via polarization modulation. *In Lasers and Electro-Optics, 2004. (CLEO)*. 2004.

9. **Fishman, D. A.** and **J. A. Nagel** (1993). Degradations due to stimulated brilouin scattering in multigigabit intensity-modulated fiber-optic systems. *J. Lightwave Technol.*, **11**(11), 1721–1728.

10. **Heismann, F.**, **P. Hansen**, **S. Korotky**, **G. Raybon**, **J. Veselka**, and **M. Whalen** (1993). Automatic polarisation demultiplexer for polarisation-multiplexed transmission systems. *Electronics letters*, **29**(22), 1965–1966.

11. **Herard, C.** and **A. Lacourt** (1991). New multiplexing technique using polarization of light. *Applied optics*, **30**(2), 222–231.

12. **H.Shankar** (2002). Duobinary modulation for optical systems. *Inphi Corporation White paper*. URL `http://www.inphi.com/products/whitepapers/DuobinaryModulationForOpticalSystems.pdf`.

13. **J.D.Downie**, **A.B.Ruffin**, and **J.Hurleyi** (2009). Ultra-low-loss optical fiber enabling purely passive 10 gb/s pon systems with 100 km length. *Optics express*, **17**(4), 2392–2399.

14. **Jopson, R. M.**, **L. Nelson.**, **G.J.Pendock**, and **A.H.Gnauck**, Polarization-mode dispersion impairment in return-to-zero and nonreturn-to-zero systems. *In Optical Fiber Communication Conference, 1999, and the International Conference on Integrated Optics and Optical Fiber Communication. OFC/IOOC '99. Technical Digest*. 1999.

15. **K.Kikuchi** (2011). Analyses of wavelength- and polarization-division multiplexed transmission characteristics of optical quadrature-amplitude-modulation signals. *Optics express*, **19**(19), 17985–17995.

16. **K.Yonenaga** and **S. Kuwano** (1997). Dispersion-tolerant optical transmission system using duobinary transmitter and binary receiver. *J. Lightwave Technol.*, **15**(8), 1530–1537.

17. **Marcuse, D.** and **C. Menyukl** (1997). Application of the manakov-pmd equation to studies of signal propagation in optical fibers with randomly varying birefringence. *J. Lightwave Technol.*, **15**(9), 1735–1746.

18. **Nelson, L. E.** and **H.Kogelnik** (2000). Coherent crosstalk impairments in polarization multiplexed transmission due to polarization mode dispersion. *Optics express*, **7**(10), 350–361.

19. **P.Boffi**, **M.Ferrario**, **L.Marazzi**, **P.Martelli**, **P.Parolari**, **A.Righetti**, **R.Siano**, and **M.Martinelli** (2008). 20-gb/s poldm duobinary transmission over 350-km ssmf supported by a polarization stabilizer and an optical dispersion compensator. *Photonics Technology Letters*, **20**(13), 1118–1120.

20. **P.M.Hill**, **R.Olshansky**, and **W.K.Burns** (1992). Optical polarization division multiplexing at 4 gb/s. *IEEE Photonics Technology Letters*, **4**(5), 500–502.

21. **Serena, P.**, *Optilux Toolbox*. University of Purma, Italy, 2009.

22. **S.Ten** and **M.Edward** (2006). An introduction to the fundamentals of pmd in fibers. *CORNING, White paper.*.

23. **T.Franck**, **T.Nielsen**, and **A.Stentz** (1996). The phase-shaped binary transmission (psbt): A new technique to transmit far beyond the chromatic dispersion limit. *ECOC 96*.

24. **T.Franck**, **T.Nielsen**, and **A.Stentz** (1997). Experimental verification of sbs suppression by duobinary modulation. *ECOC 97*, (448).

25. **Wang, C.**, **C. Wei**, **C. Lin**, and **S.Chi** (2012). Direct-detection polarization division multiplexed orthogonal frequency-division multiplexing transmission systems without polarization tracking. *Optics Letters*, **37**(24), 5070–5072.

26. **Z.Wang**, **C.Xie**, and **X. Ren** (2009). Pmd and pdl impairments in polarization division multiplexing signals with direct detection. *Optics express*, **17**(10), 7993–8004.

27. **Z.Yu**, **X.Yi**, **Q.Yang**, **M.Luo**, **J. Zhang**, **L.Chen**, and **K.Qiu** (2013). Experimental demonstration of polarization demultiplexing in stokes space for coherent optical pdm-ofdm. *Optical Fiber Communication Conference/National Fiber Optic Engineers Conference 2013*, **21**(3), OW3B.6.